The fibrous structure of the Achilles tendon enthesis in mice and its deformation under load

Dissertation

To Fulfill the
Requirements for the Degree of
„doctor rerum naturalium“ (Dr. rer. nat.)

Submitted to the Council of the Faculty
of Biological Sciences
of the Friedrich Schiller University Jena

by Julian Sartori

Referees

1. **Prof. Dr. Martin S. Fischer, Jena**
2. **Prof. Dr. Hartmut Witte, Ilmenau**
3. **Prof. Dr. Tobias Siebert, Stuttgart**

Date of disputation: 27 November 2020

Acknowledgements

I hereby thank Martin S. Fischer for the discussions in the development of the approach, the confidence he has met me with over several years of this project and timely interventions at its end, Hartmut Witte for the discussions advancing the approach and the mechanical interpretation, for his experienced advice and for taking the time to introduce me to stress tensors, Heiko Stark and Sebastian Köhring for the close, friendly and reliable collaboration over the studies and manuscripts of this dissertation, Jörg U. Hammel and Markus Löffler for the discussions and collaboration on the advancement of the imaging, for contributing their technical experience and for support with the experiments – sometimes even in the midst of the night, and Katja Felbel and Ingrid Weiß for their skillful support in the pretreatment of the specimens, discussions of techniques and for the manufacturing of the histological slices.

I thank the teams of the two beamtimes, Benjamin Naumann, George-Philipp Franz, Agustín Jorge Elias-Costa and David Junghanns for the night shifts at the beamline, the great working atmosphere and the care and knowledge they contributed to the success of these experiments, Felix Beckmann and Alexander Hipp for their help in solving tricky technical problems at the beamline, Rommy Petersohn for technical support, Elisabeth Meier, Dirk Arnold, Ms. Brinkmann, Sabine Bischoff and Michael van der Wall for the help in the keeping and provision of the animals, that left their lives in relation to this study.

I thank Cornelius Schilling, Jörg Bossert, Christian Rode and Martin Krämer for discussing the biomechanics of tendon-bone insertions with me, Mason Dean for discussing and considering a morphological approach to enthesis function, Julián A. Balanta-Melo for insights into the entheses of the masticatory apparatus, Cassandra Turcotte for discussing the interpretation of fossil entheses, Hans Pohl, Rolf Beutel, Patrick Arnold and Peter Warth for helpful discussions, technical advice and encouragement, Karolin Engelkes for an important hint with regard to the analysis of the data, Tobias Borchert for the construction of an enthesis model, Adrian Richter and Alexander Stößel for several micro-computed tomographies, Matthias Krüger for help with the dissection, Jan Giesebrecht and Julien Roussel for testing the feasibility of the fiber tracking approach and giving access to a demo version of the software, Dorothea Seeger and Johannes Thürich for proofreading and encouragement, Lucy Cathrow and Steven Youngkin for improving the English, Sandra Rüdiger for the help with formalities during this project, and the members of the Institut für Zoologie und Evolutionsforschung for the curios and encouraging atmosphere.

Table of contents

1 Introduction

Insertions of tendons and ligaments to bone in many cases exhibit a characteristic arrangement of tissues, the fibrocartilaginous enthesis (Benjamin et al., 2002). The tendon fibers pass through an unmineralized and a mineralized fibrocartilage before reaching the bone surface (Dolgo-Saburoff, 1929). This arrangement is thought to mediate between the extremely different mechanical properties of tendon or ligament on one hand and bone on the other hand (Schneider, 1956). The assumption that an immediate transition between soft and hard tissues would lead to stress singularities and necessitates mediation stems from the experience with connections between soft and hard materials in engineering. Below, some of the problems known from engineering will be summarized. Based on the structure and biomechanics of tendon, phenomena that could cause local stress maxima at the interface of soft and hard tissues are identified. These phenomena hint to the question how the structure found at the enthesis and the mechanical behavior of unmineralized fibrocartilage can lead to a homogeneous distribution of stress and inhibit premature failure.

A question from textile engineering

Connections of polymer ropes to rigid frameworks do not just experience the tensile stress transferred by the rope, but also compressive stress resulting from contact with the hard material. The superimposition of stress leads to a higher equivalent stress at the connection (Holschemacher et al., 2016). The rope has to be dimensioned according to the higher transition stress instead of the lower stress occuring along its free length (Fig. 1A). The design of rope terminations causing minimal transition stress promises weight and energy savings in conveyor technology and textile construction.

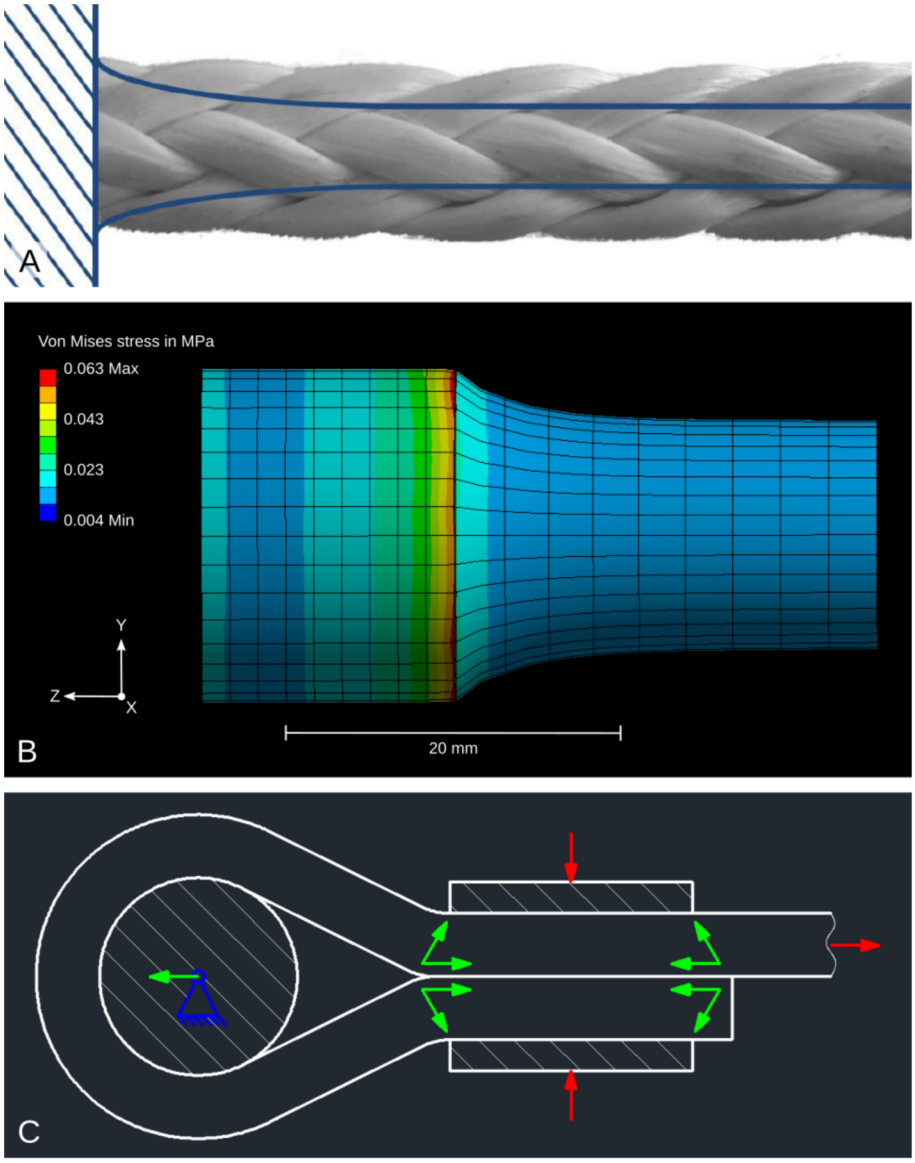

Figure 1: Hard-soft transitions lead to stress maxima.
(A) The stress occuring over a simplified hard-soft transition illustrates the necessity to over-dimension a rope.
(B) Finite element simulation of the connection between a hard (left) and a soft material (right) under tensile load in z-direction. Peak stress at the interface can be observed.
(C) Sketch of a lengthwise section through a rope termination with a rope eye and a clamp. Red arrows illustrate the applied forces, green arrows the reaction forces. The transferred tension and the compression exerted by the thimble are superimposed near its margins.
A–C by courtesy of Sebastian Köhring, C is adapted.

A sketch of a rope in a rope eye and a clamp with the transferred forces illustrates the basic problem delineated above (Fig. 1C). But transition stress does also occur in cases in which the rope is not bent around a rigid structure or compressed within a clamp. A common problem is the transfer of tensile loads across a transition in material stiffness. Under tension a compliant material exhibits high strain and usually transversal contraction. But at the transition, the stiff material constrains the deformation of the compliant material and accumulates stress in return (Fig. 1B). The terms “stiff” and “hard” will be treated as synonyms in the following text although such a simplification would be wrong in other contexts. The same applies to the terms “compliant” and “soft”. The mechanics of transitions between materials with different material properties have been explored in detail in several simple cases (Bogy, 1968; Munz & Yang, 1992; Balijepalli et al., 2016). Differences in

shear behavior and transversal contraction contribute to the resulting stress singularities. The question behind this project is whether these mechanical phenomena also occur in hard-soft transitions in biology. The objective is to identify parameters in the structure and distribution of material properties, that could mitigate stress singularities.

Motivations for research into enthesis biomechanics

The biomechanics of fibrocartilaginous entheses is of interest to various fields besides biomimetics. (1) Surgical repairs of ruptured entheses and the subsequent healing processes do not yet lead to a regeneration of graded transitions (Jensen et al., 2018). (2) In interface tissue engineering, design parameters of scaffolds have to be selected in a way that enables the regeneration of a robust tissue structure (Lu & Thomopoulos, 2013). Understanding the biomechanics of healthy entheses will help to identify the relevant structural properties and to develop surgical methods and tissue engineered constructs to recover them. (3) It will also provide context for the mechanobiology of entheses (Wang, 2006), which is itself clinically relevant, and (4) contribute to the etiology of medical conditions caused by over-use or over-loading (Barfred, 1973). As an outcome, recommendations for sports and rehabilitation could be elaborated. (5) Entheses are informative for palaeontologists. The structure of fossil bones might exhibit correlates of loading history (as specified by Carter, 1987; Carter et al., 1998). Biomechanics and mechanobiology of entheses could uncover such relations (Walters et al., 2019; Turcotte et al., 2020) and help elucidate behavioral variety within and among fossil osteichthyan populations.

Tendon insertions to bone

Entheses are regions within the locomotor system where tensile forces are transmitted between dense regular connective tissues, like tendons or ligaments, and bone. The stiffness of bone, approximated by the Young's modulus (Rho et al., 1993), is up to two orders of magnitude higher than that of tendon (Stabile et al., 2004; Liu, 2012). In spite of the problem with hard-soft transitions in engineering, clinical data shows that the enthesis is not the most common site of failure in a muscle-tendon unit (Jozsa et al., 1989). Entheses are classified as fibrous or fibrocartilaginous according to the histological appearance of the tissue at the interface with bone (Benjamin et al., 2002). Fibrous entheses mainly occur where tendons and ligaments insert to the diaphyses and metaphyses of long bones. Their structure partly relates to the necessity to migrate during growth in order to maintain a stable relative position along the bone (Dörfl, 1980).

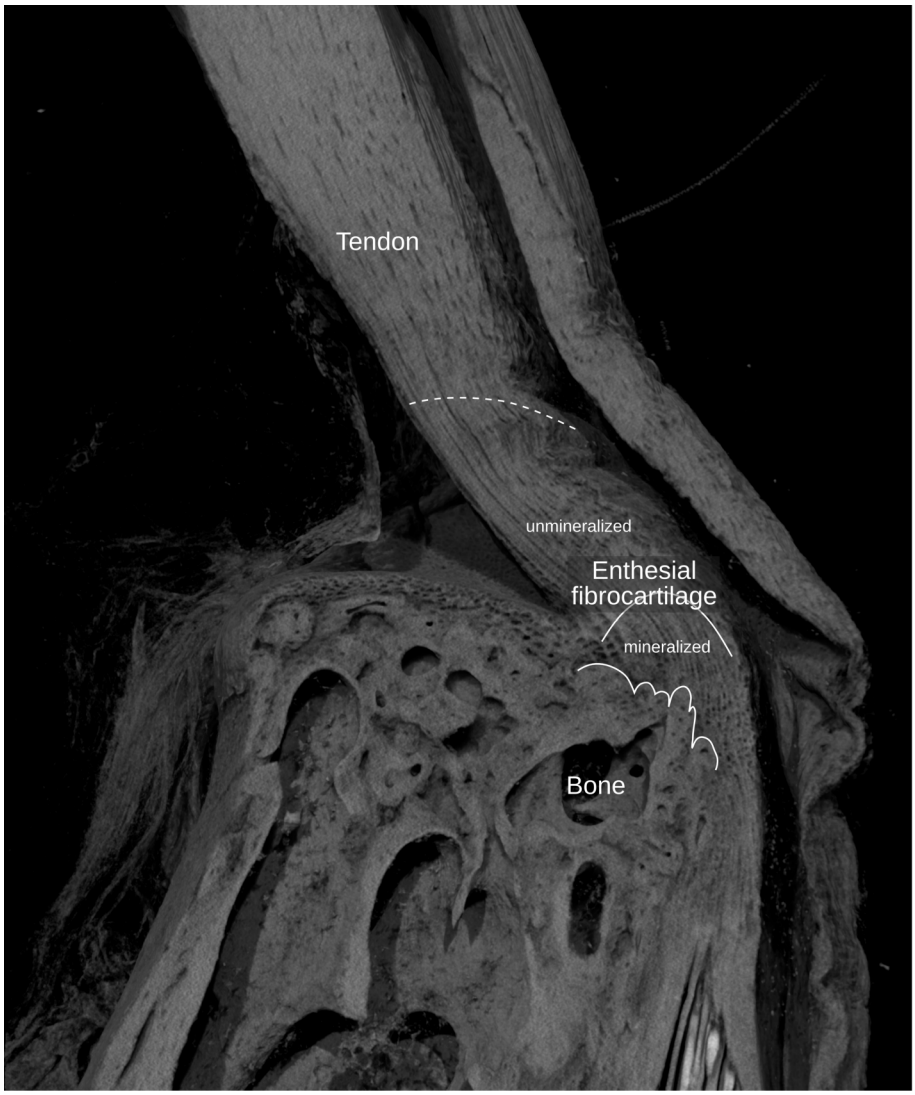

Figure 2: Histological zones of a fibrocartilaginous enthesis labelled in a volume rendering of the Achilles tendon enthesis of a mouse.

Fibrocartilaginous insertions in the limbs are situated near the ends of bones and hence in the neighborhood of the articulation (Benjamin & Ralphs, 1998). In fibrocartilaginous entheses, the transition between tendon or ligament and bone does not occur abruptly. The collagen fibers instead pass through unmineralized and mineralized fibrocartilage (Fig. 2) in which the composition and structure of the extrafibrillar matrix gradually change (Benjamin & Ralphs, 1998; 2000; Thomopoulos et al., 2003; Schwartz et al., 2012; Kuntz et al., 2018) before their fibers separate into fibrils that seem to be continuous with the collagen fibrils of bone (Zhao et al., 2014). Fibrocartilaginous entheses were selected as the research object of this project because they appeared as an ideal example of tensile stress transfer over a transition from soft to hard tissues.

Multiscale tendon biomechanics

The focus of this study is on tendon entheses. Therefore, in the following section details of tendon biomechanics will be described. Most statements are as well applicable to ligaments. The terminology used was established by Handsfield et al. (2016). The term “fibrous components” is used as an umbrella term for fascicles, fibers, fibrils and microfibrils.

The response of tendon in a tensile test leads to a characteristic stress-strain curve that can be subdivided into three parts (Wang, 2006; Ker, 2007). (1) In the initial toe region, stress increases modestly with strain. (2) It is followed by a steeper linear elastic response. (3) Before ultimate specimen failure, the curve flattens again.

Additionally, time-dependent viscoelastic behavior is found (Butler et al., 1978). The tendon response is strain-rate dependent. Hysteresis, creep and relaxation are observed. Because tendon is a hierarchical tissue, its macroscopic deformation results from deformations at multiple levels of its organization.

The fibrous components of tendon, like fascicles and fibers, are not perfectly aligned with the tendon course in the relaxed state. Therefore, substantial fiber realignment is observed during preconditioning and tendon elongation (Lake et al., 2009; Miller et al., 2012c). On one hand, deviation from the tendon axis occurs due to apparently unordered orientations of fibers in the relaxed state. On the other hand, fascicles are known to follow helical courses within tendons (Kalson et al., 2012; Thorpe et al., 2013). The components of a stretched helix are compressed against each other upon load application (Reese et al., 2010). Furthermore, collagen fibrils exhibit a characteristic crimp pattern, which is also a form of deviation from the loading direction. Uncrimping, an alignment of the fibrils, mainly occurs in the toe-region of the stress-strain curve (Diamant et al., 1972; Franchi et al., 2007; Miller et al., 2012a).

Micromechanical examinations find sliding among neighboring fibrils (Connizzo et al., 2014; Szczesny & Elliott, 2014), fibers (Screen et al., 2004) and fascicles (Thorpe et al., 2012; 2015) and shearing of the matrix between them. Sliding among fibers and fascicles is reversible. In fascicle sliding reversibility is brought about by elasticity of the interfascicular matrix (Thorpe et al., 2015). The stiffness of the interfascicular matrix has a strong influence on overall tissue behavior (Thorpe et al., 2012). Fibril and fiber sliding are major factors for fascicle relaxation, the matrix between them shows a viscoelastic response to shearing (Screen, 2008; Gupta et al., 2010; Szczesny & Elliott, 2014). Recent studies also showed that shearing of the matrix generates pressure in its liquid

phase and leads to liquid flow – a poroelastic behavior (Ahmadzadeh et al., 2015; Connizzo & Grodzinsky, 2017; 2018).

Mechanical models explaining how sliding can lead to the macroscopic tissue response are based on the assumption that fibrils have a finite length much shorter than the tendon (Szczesny & Elliott, 2014; Ahmadzadeh et al., 2015). Tensile loading of fibrils is thought to occur due to relative sliding of neighboring fibrils and shear of the matrix between them. The same assumptions could be required in fibers. However, structural studies find continuity of fibrils and fibers along tendons (Birk et al., 1989; 1997; Provenzano & Vanderby, 2006; Edama et al., 2015; 2016; Svensson et al., 2017). But not only fibers and fibrils of finite length can slide. All kinds of realignment of fibrous structure and even deformation of helical arrangements could lead to sliding among the involved fibrous components. Studies visualizing the fibrous structure of macroscopically large tissue regions during deformation could contribute to the resolution of this contradiction.

As fibrils are comparatively stiff, fibril strains are low in the toe region of the tensile response of the tissue. But at the end of the linear region they can amount to up to 50 % of tissue strain (Sasaki & Odajima, 1996; Puxkandl et al., 2002; Rigozzi et al., 2011). The deformation of fibrils in a physiological range is thought to be a combination of uncoiling of the molecular helix and sliding among molecules (Sasaki & Odajima, 1996; Fratzl et al., 1998; Rigozzi et al., 2011; Depalle et al., 2015).

The mechanical behavior of a specific tendon depends on various structural and compositional parameters because of the multiscale character of tendon deformation. The comparison of energy-storing and positional tendons (Ker et al., 1988; Alexander, 2002; Thorpe et al., 2012; 2013; Birch et al., 2013; Screen et al., 2013; 2015) has become a productive approach for research into structural based models of tendon biomechanics. Even the fibrils of energy-storing and positional tendons differ with regard to their stiffness (Quigley et al., 2018). The differences are caused by different degrees of cross-linking among the collagen molecules. Further factors that can increase fibrillar stiffness are dehydration and mineralization (Sherman et al., 2015).

In the project reported here, the focus is on the fiber level. At present, fibers are the smallest entity that can be three-dimensionally visualized over a complete tendon because the achievable spatial resolutions are limited by specimen size in many imaging techniques. This approach follows a “from rough to detail” philosophy and allows analogies with fiber based constructs in engineering. However, a “fiber” is not very well defined in a mechanical sense. The crimping state of the

comprised fibrils, the helical pitch of fibrils and microfibrils, as well as the cross-linking of the collagen molecules are obscure at this level of observation. These parameters can vary within and among fibers – and each parameter has profound effects on the mechanical behavior of the fiber.

Entheseal fibrocartilage

Fibrocartilage is considered to be a major factor in the robustness of fibrocartilaginous entheses. Enthesial fibrocartilage can be divided into two types according to its composition and structure: unmineralized and mineralized fibrocartilage (Dolgo-Saburoff, 1929).

Unmineralized fibrocartilage in tendons and ligaments develops through tissue metaplasia from dense regular connective tissue (Gao et al., 1996; Galatz et al., 2007). Metaplasia can also be induced by subjecting a tendon to compressive stress (Malaviya et al., 2000). Fibrocartilage development is explained theoretically with load histories involving tensile strain and superimposed hydrostatic compressive stress (Carter, 1987; Carter et al., 1998).

At entheses the transition between tendon and fibrocartilage is gradual. It is remarked histologically by the increasing sphericity of cells in the fibrocartilage (Cooper & Misol, 1970). Like in tendon tissue the cells are usually aligned in rows parallel with the collagen fibers. Fibrocartilage cells in contrast with tendon fibroblasts (McNeilly et al., 1996) do not maintain a network of cell processes connected by gap junctions (Ralphs et al., 1998). A study of the transcriptome of tendon, fibrocartilage and articular cartilage concluded that fibrocartilage cells undergo a partial cartilage differentiation (Kuntz et al., 2018). Fibrocartilage cells generate a pericellular and a territorial matrix around them (Benjamin & Ralphs, 2004). These matrix regions, and one or several cells contained in it, together form a chondron. The extracellular matrix of fibrocartilage differs from that of tendon in several structural and compositional aspects. The collagen fibers that are continuous with those of the tendon contain a relevant share of collagen type II (Rufai et al., 1992; Benjamin & Ralphs, 1998; Waggett et al., 1998; Rossetti et al., 2017). An important difference between collagen type I and type II is that type II contains chemical groups mediating the interaction with proteoglycans (Gelse et al., 2003). Especially the proteoglycan aggrecan is found in fibrocartilage but not in tendon (Waggett et al., 1998). Its glycosaminoglycan molecules were found to exhibit a regular orientation relative to the axis of collagen fibers (Vidal et al., 2015). The regularity is as well indicative of the stabilizing effect of interactions between the collagen and the glycosaminoglycan chains. Poroelasticity is in two ways related to the presence of proteoglycans in the tissue: Their negatively charged glycosaminoglycan chains bind high amounts of water (Kiani et

al., 2002). When densely packed, they also reduce the tissue permeability (Nia et al., 2015). The biomechanical similarity between fibrocartilage and articular cartilage seems to be high. Articular cartilage is modeled as a biphasic material with fixed charges leading to osmotic swelling and a porosity that is reduced with compression (Klika et al., 2019). Fibrocartilage is as well considered very similar to hydrogels – an analogy used for biomimetics (Liu et al., 2020) and for modeling the cellular environment of cartilage cells.

At the transition between unmineralized and mineralized fibrocartilage several studies found a region that is more compliant than either tendon or bone (Sano et al., 2006; Deymier et al., 2017; Locke et al., 2017; Rossetti et al., 2017). Models by Connizzo et al. (2016) explain the higher compliance of the insertion with a less organized structure. Models that also take into account the mineralization suggest that the superimposition of a high angular deviation of fibrils near the insertion and mineralization below a percolation threshold leads to a reduction of tissue stiffness (Liu et al., 2014). But it is completely unclear how a compliant region could contribute to the mitigation of stress concentrations near the insertion. The only model attempting to explain this is based on the rotator cuff and requires a stiffer ring on the tendon side of the compliant zone that facilitates tangential stress transfer around the insertion (Liu et al., 2012). These structural requirements do not occur in other entheses – and their agreement with the conditions at the rotator cuff may be questioned.

Mineralized enthesial fibrocartilage develops through the mineralization of unmineralized fibrocartilage (Schwartz et al., 2012). The tidemark, a relatively smooth, basophilic layer, corresponds to the mineralization front (Cooper & Misol, 1970; Rufai et al., 1996). However, the transition between unmineralized and mineralized fibrocartilage is not completely abrupt: the mineralization increases along a gradient in mineral content and mineralization pattern (Wopenka et al., 2008; Schwartz et al., 2012) that extends over tens of micrometers in a mouse (Deymier-Black et al., 2015). Apatite crystals accumulate within and between fibrils (Landis et al., 1996; Schwartz et al., 2012). Above a percolation threshold the increase also results in a gradual increase in tissue stiffness (Liu et al., 2014). In engineering, similar gradients are among the obvious solutions to the mechanical problems of compliant-stiff transitions (Libanori et al., 2012), mitigating any accumulation of tensile or transition stress by distributing the transition stress over the length of the gradient.

During growth, mineralized fibrocartilage is replaced by bone at the tissue interface. The enthesis is therefore considered to be a growth plate, and its development a halted ossification process (Schneider, 1956; Gao et al., 1996). Tendon fibers can be traced through the enthesis up to the interface where mineralized fibrocartilage and bone meet (Clark & Stechschulte, 1998; Benjamin et al., 2002; Milz et al., 2002). The collagen fibrils are straight within the mineralized fibrocartilage and do not exhibit crimp (Clark & Stechschulte, 1998). At the interface with bone the fibers dissociate. But in the porcine anterior cruciate ligament, the fibrils go on (Zhao et al., 2014). On the fibrillar level, tendon and bone could be continuous. The transition to bone is accompanied by an increase in tissue stiffness by one order of magnitude (Mente & Lewis, 1994). At the interface, mineralized fibrocartilage and bone are highly interdigitated (Benjamin et al., 1986; 2006; Milz et al., 2002). As Schneider (1956) pointed out, interdigitations of dissimilar materials deform in a way that increases the contact area under shear load, which is the main load case of this interface.

Mineralized fibrocartilage is considered a hard tissue. Its deformation under physiological loads can barely be registered on a microscopic scale. This project mainly focused on the soft tissues of the enthesis and the question how their much larger deformations lead to a homogeneous distribution of stress across them and along the transition from tendon to the mineralization front.

Functions of fibrocartilaginous entheses

The anatomical context of fibrocartilaginous entheses is important to understand their function. They are not usually situated on the bone surface that faces the inserting tendon. Rather, the tendon approaches the surface obliquely or near tangentially, to insert at the side or end of the bone, remote from the corresponding joint (Benjamin et al., 2006). This leads to force transmission with a maximized lever arm, as well as to contact between tendon and bone before the attachment. The pressure between the tendon and the surface of the bone depends on the transferred tensile force. In many cases the contact is mediated by a periosteal cartilage overlying the bone, a sesamoid fibrocartilage in the tendon and a bursa between these mediating structures (Barfred, 1973; Rufai et al., 1995). These tissues are thought to protect tendon and bone from damage due to the compression. Mechanically, their arrangement is thought to function like a segment of a pulley. Together with the transitional tissues of the insertion, they are termed the enthesis organ (Benjamin & McGonagle, 2001). In a few entheses, a tongue-like fat pad slides into the bursa at certain insertion angles (Canoso et al., 1988), acting as a soft and dynamic spacer. The position of most fibrocartilaginous insertions near the ends of bones, and hence in the neighborhood of the

articulation (Benjamin & Ralphs, 1998), leads to a variation of insertion angle and area of contact between tendon and bone with joint angle.

The load case of many insertions is dynamic, with cyclic changes in tensile stress and joint angle if the tendon is involved in locomotion (Fischer et al., 2002). Loads can be extreme, in the Achilles tendon they can reach ten times the body weight (Ashton-Miller et al., 1992). Many tendons do not just transfer tensile loads but also contribute to energy-storage (Ker et al., 1988) and attenuation of peak loads.

Because the compliance of a muscle-tendon unit is so clearly confined at the mineralization fronts at its origin and its insertion, a homogeneous distribution of stress within its cross-sections has to be provided by inherent mechanisms. A homogeneous distribution of stress is equivalent with the recruitment of all components in load transfer. From an adaptionist perspective, the following expectations could be formulated: A near homogeneous distribution of stress across the tendon should be achieved at maximum load. At common loads, the distribution should be sufficiently homogeneous to prevent local damage and over-use.

Hypothetical mechanisms leading to a homogeneous distribution of stress across the muscle-tendon unit have to be robust with regard to three factors.

(1) The length that is elongated between origin and insertion can differ between the superficial and the deep muscle-tendon unit (Fig. 3A). The superficial fibers of the Achilles tendon for example reach further distal than the deep fibers. Such a configuration is expected to lead to lower stress in the superficial fibers, because of their higher initial length.

(2) As described above, the angle at which a tendon approaches the bone varies with the joint angle. For geometric reasons, a change in attachment angle leads to a differential displacement of fibrous tendon components dependent on the distance from the center of rotation. However, the variation in attachment angle is mitigated by bony pulleys and *retinacula*. Furthermore, the enthesis might only be able to withstand maximum loads within a restricted range of attachment angles.

(3) The duration of load application can vary. At bony pulleys, the tendon exhibits fibrocartilages. The response of fibrocartilages to compression shows a poroelastic component (Connizzo & Grodzinsky, 2017). Accordingly, the compression of a fibrocartilage depends on the duration of load application. As the tendon structure is curved at the pulley, a compression of the fibrocartilage will lead to differential displacements between deep and superficial fibrous components (Fig. 3B).

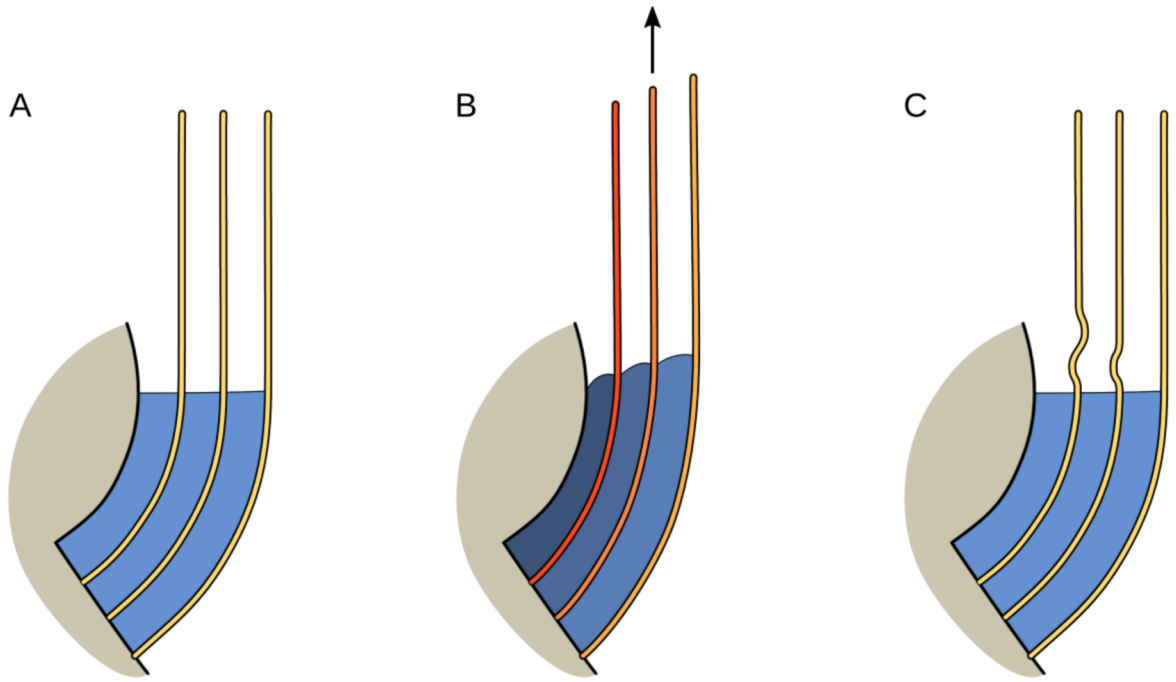

Figure 3: Differential elongation due to tendon curvature around a bony pulley. (A) Arrangement in the relaxed state and (B) under load. (C) Differential reserve lengths could compensate the effect.

Besides the functions treated thoroughly in this text, the enthesis has to maintain its cellular population. The cells are involved in the development of the tissue during growth, adaptation, remodeling and healing.

Hypotheses of enthesis biomechanics

Five possible mechanisms that could contribute to a homogeneous distribution of stress across the tendon can be formulated out of geometric and mechanical considerations. A combination of these mechanisms is expected to occur.

(1) The reserve lengths in the relaxed state could be inhomogeneous between groups of fibrous components (Thambyah et al., 2014) so that homogeneous recruitment is achieved at maximum load (Fig. 3C). This principle could compensate for differences in initial length, for example between the deep and superficial tendon. But it can neither balance changes in insertion angle, nor differential elongation due to the compression of the fibrocartilage over time. (2) Differential contraction among the motor units in the muscle that are connected to different portions of the tendon could lead to stretching of loose portions and to the release of taut ones. A structural requirement for muscular control of the stress distribution is that different motor units have to be

connected to those portions of the tendon that experience differential stress. (3) Fibrous components of the tendon exert pressure onto the matrix between them under load according to their curvature (Giori et al., 1993), for example at pulleys. The incompressible liquid in the matrix is pressed out against the resistance of a low tissue permeability (Wren et al., 2000). The stress in the fibrous components could be homogenized because the pressure in the liquid phase would cause compensating flows of liquid locally. (4) Fibrous components in helical arrangements are compressed against each other (Cummins et al., 1946; Reese et al., 2010) which leads to a homogenization of stress among them. However, as soon as fibers are straightened within a helical arrangement they cannot contribute to a further homogenization. (5) Shear among fibrous components also leads to a transmission of stress across the tendon.

Contributions to a homogeneous distribution of stress across the tendon can occur along the complete muscle-tendon unit. Understanding how they work and what kind of stress distribution they achieve is a prerequisite for an understanding of the hard-soft transition. Principles that mediate between the loading regimes and the deformation mechanisms of tendon and bone are primarily assumed to occur near the transition – within the enthesis.

The most obvious mechanism contributing to a mediation of hard and soft tissues is the mineralization gradient. However, the gradient is too short to explain a mediation of tissue level deformation. Instead, its hypoallometry (Deymier-Black et al., 2015) suggests that it might mediate the transition from soft to hard at the fibril level.

The finding of a zone in the enthesis that is more compliant than either tendon or bone (Deymier et al., 2017; Rossetti et al., 2017) challenges the idea of the enthesis as a structure that mediates between hard and soft tissues. Genin and Thomopoulos (2017) posit that toughness of the enthesis is central to its function. Yet, there are no structural or compositional correlates of a higher strength of the compliant region. Therefore, the question how stress maxima resulting from the transition between hard and soft are avoided remains. A two-sided approach to this problem was followed: On one hand the third study of this project pursued the reexamination of the compliant zone in intact specimens. On the other hand, the unmineralized fibrocartilage was examined with regard to structure and deformation. The question behind this second part is, whether the deformation mechanism of fibrocartilage would lead to similar stress singularities at the tissue level as suggested by theoretical models of simplified transitions between hard and soft materials in engineering (Bogy, 1968; Munz & Yang, 1992; Balijepalli et al., 2016).

A classic model hypothesized that unmineralized fibrocartilage would function as a “stretching brake” (Knese & Biermann, 1958) or “transversal contraction brake”. In anatomy textbooks, this function is commonly depicted (Schünke, 2014) as fibers which loop over cartilage chondrons and deform the chondrons whenever the structure is stretched under tension. In such a configuration, the material properties of the chondrons influence the stiffness or damping of the transition zone. Increases in number or sphericity of chondrons could lead to a gradient, that would mediate between the different deformation behaviors of tendon and bone. Benjamin et al. (2002) modified the model by suggesting that not chondrons but water bound by aggrecan could lead to a modification of tissue bending stiffness and transversal contraction behavior towards the insertion to hard tissue. Wren et al. (2000) modeled fibrocartilage in a wrap-around tendon as a poroelastic material. They were able to show that in a fibrocartilage with adaptive permeability the liquid phase would bear compressive stress at the onset of loading. Compressive stress would only be transferred to the solid phase as the pressurized liquid evades over time. According to this model, the lowest permeability should be found where the tendon is compressed against a pulley. Recent studies found evidence for poroelastic behavior of tendon and fibrocartilage (Connizzo & Grodzinsky, 2017; 2018). They found the permeability in murine Achilles tendons to be higher near the insertion than in the free tendon. The authors concluded that permeability might be more related to collagen morphology than to the presence of aggrecan. But in their experiment the bony pulley was removed. Based on the fact that tissue porosity decreases with compression (Klika et al., 2019), the low permeability near the insertion might be an artifact. The state of the art is therefore still contradictory with regard to fibrocartilage biomechanics. However, these studies make clear that fibrocartilage transversal contraction is different from the transversal contraction in many engineering materials. Fibrocartilage that transfers tensile stress is under pressure because of its deformation mechanism (Ahmadzadeh et al., 2015). Therefore, the projected stress singularities, due to a mismatch in transversal contraction, might not exist. This hypothesis necessitates the examination of the structure and deformation of the fibrocartilage near the interface.

The previous discussion has a ramification with regard to the stress experienced by single fibers. A fiber bent sharply at the soft-hard transition would exhibit extreme local stress due to compression and bending. The classic model of fibrocartilage included the notion that fibrocartilage could protect fibers from such a deformation by its bending stiffness that would shield fiber bending away from the hard tissue (Schneider, 1956; Benjamin et al., 1986; Benjamin & Ralphs, 2000). Schneider (1956) has compared this function to that of a grommet on a plug. Localized fiber bending might to

some extent be mitigated by the mineralization gradient. But the short length of the gradient cannot prevent an increase in stress. Recent studies in sliced entheses found a very high curvature of the fibers near the insertion (Sevick et al., 2018). The models of fibrocartilage function that were discussed above suggest that fibrocartilage can only prevent sharp bending of fibers over a restricted time. This is another case that requires a reexamination by a deformation study of intact specimens – and research with regard to the structure and biomechanics that lead to the found deformation behavior.

Approach

In vivo (enthesial) biomechanics evades direct examination because of a lack of techniques for noninvasive, high-resolution, three-dimensional imaging and stress measurement (Disney et al., 2018). It is indirectly approximated by studies of *ex vivo* tissue structure, composition, deformation and material properties (Zhao et al., 2014; Deymier et al., 2017; Rossetti et al., 2017), by low-resolution *in vivo* imaging and measurements (Han et al., 2014), by the epidemiology of enthesis injuries (Yu & Yu, 2015), as well as by invasive studies in model systems (Thomopoulos et al., 2015). The described homogenization mechanisms and ideas of fibrocartilage biomechanics have structural requirements. Many of them can be evaluated at a microscopic scale. This projects combines examinations of the tissue structure and mechanical experiments to test the formulated hypotheses and narrow down enthesial biomechanics. Structural and mechanical investigations were both based on high-resolution three-dimensional imaging. In terms of structure, the focus was on fibers.

The Achilles tendon insertion in mice

The insertion of the Achilles tendon is a representative example of a fibrocartilaginous enthesis. Together with the sesamoid fibrocartilage, the periosteal cartilage, the bursa between them and Kager's fat pad protruding into the bursa, it embodies the idea of an enthesis organ (Benjamin & McGonagle, 2001) and was termed the "premiere enthesis" for this reason (Canoso, 1998). At the same time, it is accessible to dissection and imaging. In micro-computed tomography the achievable spatial resolution depends on specimen size. Fiber size seems to show negative allometry with body size (Handsfield et al., 2016). Consequently, a better resolution of the fibers can be achieved in small animals. I chose to examine the Achilles tendon enthesis in mice (*Mus musculus*) because the literature on this structure is comprehensive enough to provide sufficient context at the same time.

The Achilles tendon is an energy-storing tendon in most mammals (Alexander, 2002; Birch et al., 2013) that engage in terrestrial locomotion. In small mammals many tendons are not subdivided into fascicles by endotenon (Benjamin & Ralphs, 1998). The applied imaging methods allow to study the fibers of the Achilles tendon in mice within their intact anatomical context, the muscle-tendon unit of the *M. triceps surae*. Therefore, the macroscopic context is well defined.

2 Overview of the manuscripts

Three-dimensional imaging of the fibrous microstructure of Achilles tendon entheses in *Mus musculus*

Sartori, J., Köhring, S., Witte, H., Fischer, M.S., Löffler, M., 2018, Journal of Anatomy 233, 370–380.

The article summarizes the testing of protocols for contrast-enhancement of connective tissues in micro-computed tomography. By a combination of a histological technique for scanning electron microscopy and propagation-based phase-contrast the fibrous structure of Achilles tendon entheses in mice was visualized and qualitatively described. A spatial reference system was developed to measure structural parameters at defined longitudinal tendon positions and compare them among specimens.

J.S., S.K., H.W. and M.S.F. designed the study. J.S. and M.L. planned the investigations. M.L. and J.S. acquired the data. J.S. analyzed the data. J.S., M.L. and S.K. interpreted the results. J.S. wrote the manuscript. M.L., S.K., H.W. and M.S.F critically reviewed the manuscript. J.S. contributed 70 % to the overall work of this study.

Tracking tendon fibers to their insertion – a 3D analysis of the Achilles tendon enthesis in mice

Sartori, J., Stark, H., accepted 06 May 2020, Acta Biomaterialia.

Fibers were tracked in volume images of the fibrous structure from the first study. Fiber courses and volume images were analyzed with regard to mechanically relevant parameters of the fibrous structure. The results show that the strength of the enthesis cannot be explained with structural reinforcement.

J.S. designed the study. H.S. and J.S. developed computational methods for fiber analysis. J.S. analyzed the data. J.S. and H.S. interpreted the results. J.S. and H.S. wrote the manuscript. H.S. critically reviewed the manuscript. J.S. contributed 75 % to the overall work of this study.

Gaining insight into the deformation of Achilles tendon entheses in mice

Sartori, J., Köhring, S., Hammel, J.U., in prep., Advanced Engineering Materials.

This manuscript reports the examination of entheses in a tensile test that was mounted in a synchrotron beamline. The resulting volume images were used to measure strain and volume changes, as well as to evaluate structural changes. Critical parameters for the advancement of the method were identified.

J.S. and J.U.H. designed the study. J.S., J.U.H. and S.K. planned the experiments. S.K. developed the testing device. J.S. prepared the specimens. J.S., S.K. and J.U.H. acquired the data. J.S. and J.U.H. analyzed the data. J.S. interpreted the results. J.S. wrote the manuscript. J.S. contributed 80 % to the overall work of this study.

3D imaging the fibrous microstructure of Achilles tendon entheses in *Mus musculus*

Julian Sartori[1] Sebastian Köhring,[2] Hartmut Witte,[2] Martin S. Fischer[1] and Markus Löffler[3]

[1] Institut für Zoologie und Evolutionsforschung, Friedrich-Schiller-Universität Jena

[2] Fachgebiet Biomechatronik, Fakultät für Maschinenbau / IMN MacroNano®, Technische Universität Ilmenau

[3] Dresden Center for Nanoanalysis (DCN), Center for Advancing Electronics Dresden (cfaed), Technische Universität Dresden

Abstract

The whole-organ, three-dimensional microstructure of murine Achilles tendon entheses was visualized with micro-computed tomography (microCT). Contrast-enhancement was achieved either by staining with phosphotungstic acid (PTA) or by a combination of cell-maceration, demineralization and critical-point drying with low tube voltages and propagation-based phase-contrast (fibrous structure scan). By PTA-staining, X-ray absorption of the enthesial soft tissues became sufficiently high to segment the tendon and measure cross-sectional areas along its course. With the fibrous structure scans, three-dimensional visualizations of the collagen fiber networks of complete entheses were obtained. The characteristic tissues of entheses were identified in the volume data. The tendon proper was marked as a segment manually. The fibers within the tendon were marked by thresholding. Tendon and fiber cross-sectional areas were measured. The measurements were compared between individuals and protocols for contrast-enhancement, using a spatial reference system within the three-dimensional enthesis. The usefulness of the method for investigations of the fibrous structure of collagenous tissues is demonstrated.

doi: 10.1111/joa.12837

Tracking tendon fibers to their insertion – a 3D analysis of the Achilles tendon enthesis in mice

Julian Sartori and Heiko Stark

Institut für Zoologie und Evolutionsforschung, Friedrich-Schiller-Universität Jena

Abstract

Tendon insertions to bone are heavily loaded transitions between soft and hard tissues. The fiber courses in the tendon have profound effects on the distribution of stress along and across the insertion. We tracked fibers of the Achilles tendon in mice in micro-computed tomographies and extracted virtual transversal sections. The fiber tracks and shapes were analyzed from a position in the free tendon to the insertion. Mechanically relevant parameters were extracted. The fiber number was found to stay about constant along the tendon. But the fiber cross-sectional areas decrease towards the insertion. The fibers mainly interact due to tendon twist, while branching only creates small branching clusters with low levels of divergence along the tendon. The highest fiber curvatures were found within the unmineralized entheseal fibrocartilage. The fibers inserting at a protrusion of the insertion area form a distinct portion within the tendon. Tendon twist is expected to contribute to a homogeneous distribution of stress among the fibers. According to the low cross-sectional areas and the high fiber curvatures, tensile and compressive stress are expected to peak at the insertion. These findings raise the question whether the insertion is reinforced in terms of fiber strength or by other load-bearing components besides the fibers.

doi: 10.1016/j.actbio.2020.05.001

Gaining insight into the deformation of Achilles tendon entheses in mice

Julian Sartori[1], Sebastian Köhring[2], Stefan Bruns[3], Julian Moosmann[4] and Jörg U. Hammel[4]

[1] Institut für Zoologie und Evolutionsforschung, Friedrich-Schiller-Universität Jena

[2] Fachgebiet Biomechatronik, Fakultät für Maschinenbau / IMN MacroNano®, Technische Universität Ilmenau

[3] Institute of Metallic Biomaterials, Helmholtz-Zentrum Geesthacht

[4] Institute of Materials Physics, Helmholtz-Zentrum Geesthacht

Abstract

Understanding the biomechanics of tendon entheses is fundamental for surgical repair and tissue engineering, but also relevant in biomimetics and palaeontology. 3D imaging is becoming increasingly important in the examination of soft tissue deformation. But entheses are particularly difficult objects for micro-computed tomography because they exhibit extreme differences in X-ray attenuation. In this article, the ex vivo examination of Achilles tendon entheses from mice using a combination of tensile tests and synchrotron radiation-based micro-computed tomography is reported. Two groups of specimens with different water content are compared with regard to strains and volume changes in the more proximal free tendon and the distal tendon that wraps around the Tuber calcanei. Tomograms of relaxed and deformed entheses are recorded with propagation-based phase contrast. The tissue structure is rendered in sufficient detail to enable manual tracking of patterns along the tendon, as well as 3D optical flow analysis in a suitable pair of tomograms. High water content is found to increase strain and to change the strain distribution among proximal and distal tendon. In both groups, the volume changes are higher in the distal than in the proximal tendon. These results support the existence of a compliant zone near the insertion. They also show that the humidity of the specimen environment has to be controlled. Necessary steps to extend the automatic tracking of tissue displacements to all force steps are discussed.

doi: 10.1101/2021.01.23.427898

3 Discussion

The studies of this project combined methodological advancements with structural and biomechanical examinations of the Achilles tendon enthesis in mice. The following text will first discuss the methodological contributions, then summarize the structural findings of the studies into a larger image and combine them with the study of enthesis deformation to deduce a model of enthesis biomechanics. Finally, the overall approach will be discussed.

Methodical advancements

Over two studies, a workflow for the three-dimensional examination of the fibrous structure of connective tissues was established comprising five steps. The workflow is based on a novel combination of (1) histological protocols and (2) techniques for 3d imaging of the fibrous structure. (3) An established method for fiber tracking is applied to the resulting volume images, which is the first published application to tendon data. (4) The fiber tracks are quantitatively analyzed using custom software with features that were partly developed for the study. (5) Measures from the analysis are summarized within a spatial reference system that is developed according to the anatomical structure examined.

The first two steps were validated by a comparison to histological slices. The agreement between measures from the analysis of the fiber tracks and the literature lends credibility to fiber tracking and analysis. Results from the analyses and the volume data can be combined within three-dimensional renderings so that specimen morphology and quantifications can be compared.

The spatial reference system developed for the Achilles tendon enthesis in mice allows comparison of results across individuals and methods. It was used to compare results from an analysis of cross-sections to data from the fiber analysis. Even measurements of cross-sectional areas and strains from the deformation study in a synchrotron beamline can be summarized within the spatial reference system. In this way, the spatial reference system provides the basis for the development of structurally-informed models of the enthesis. It could as well enable the comparison across species.

The deformation experiments benefited from a combination of soft tissue imaging, a custom tensile testing device and dissection protocols keeping the mechanically relevant structures of the enthesis intact. From this combination, visualization of the *ex vivo* three-dimensional structure, in a mechanically defined state under physiological conditions, without chemical treatment and at a high

spatial resolution were achieved. Like in the fibrous structure study, a voxel resolution below 2 µm was crucial for resolving the microscopic tissue structure. The design of the tensile testing device followed requirements for achieving mechanically and physiologically defined conditions and was subjected to the boundary conditions prescribed by the beamline. In each iteration of these experiments the setup was further optimized – and the potential for future refinements is high. The analysis of the volume data from the deformation experiments still relied on manual segmentation and pattern tracking. But at the projected higher image qualities, tracking could be automated and the data could be subjected to methods used in the fibrous structure study as well.

Importantly for the overall approach, all examinations were carried out in the same enthesis in one species. The fibrous structure known from the structural studies is subjected to a defined load in the deformation experiments.

Synopsis of the structural findings

Fiber courses

A consistent image of the fibrous structure of the Achilles tendon enthesis in mice emerges from the examinations with various methods. Volume data and fiber tracks suggest that parallel fibers with occasional branching prevail throughout the tendon from the midsubstance to the insertion. The morphological examination showed that these fibers are continuous through the mineralized fibrocartilage to the interface with bone, as well as into the origin of the *M. adductor brevis digiti minimi* that originates at the plantar side of the *Calcaneus* distal from the Achilles tendon enthesis and proceeds to the fifth digit. The rate of branching is still underestimated due to fiber tracking, for example only few fiber tracks and branching points were found in the sesamoid cartilage in spite of its richness in transversal connections.

The fibers at the margins of the tendon are wound in helices around the tendon axis with an increase of the helical angle towards the insertion. High helical angles are rather found in energy-storing tendons than in positional ones (Thorpe et al., 2013). The Achilles tendon is known to contribute to energy-storage in the terrestrial locomotion of many mammals. Interestingly, the central fibers are nearly parallel with the overall tendon course. The increase in angular deviation along the tendon could not be stable in a structure in which fibers can slide relative to one another without resistance. Consequently, the increasing angles point to interactions between the fibers that could be the result of branching or shear stiffness of the matrix. Shear stiffness is a more likely candidate for this

interaction, because Barfred (1973) described that the co-occurrence of high helical angles and intense cross-linking among fiber is seldom. The increase of the helical angle towards the insertion predicts a higher compliance of the insertion as well as a higher recruitment of the matrix between the fibers during tensile loading. The variation of the helical angles across and along the tendon questions published findings that are based on a superficial or local measurement of the helical angle (Thorpe et al., 2013; Riggin et al., 2014).

In the distal part of the tendon the fibers curve towards the insertion. Such curvatures were consistently found in our data, but they are often neglected in mechanical studies of enthesial tissues (Connizzo & Grodzinsky, 2017; Rossetti et al., 2017). However, the small curvature radii measured in this region are a mechanically relevant parameter to calculate the pressure that the fibers exert on the neighboring matrix.

The Achilles tendon is composed of two subtendons. One of them is a union of the aponeuroses from the *M. gastrocnemius medialis* and a small part of the *M. gastrocnemius lateralis*. Fiber tracking provided cues that the fibers of this subtendon could be traced through the tendon to a protrusion of the insertion area on the *Calcaneus*. This suggestion is supported by differences in reserve lengths between this tendon portion and the rest of the tendon. These differences could result from a different reaction of the muscle portions to the histological treatment. In contrast with the increase in helical angle, differences in reserve lengths are more likely to occur when the interaction among fibers and tendon portions and the resistance against sliding among them is low.

Although fiber tracking is a rather stochastic approach for the processing of the volume data, the resulting fiber courses correspond well with the volume images with regard to fiber position, orientation and curvature. Further parameters like fiber density, branching, the positions of fiber ends and the absolute length of single fibers are not represented accurately. Due to the combination with measurements from cross-sections, a more accurate model of the fibrous structure can be achieved. The fiber tracks were published to enable reexamination of the findings and their use in other studies.

Dimensional measures of tendon and fibers

The decrease in cross-sectional area towards the insertion is a finding that was intensely discussed in both studies dealing with the fibrous structure. The native specimens of the deformation study were shown to exhibit larger cross-sectional areas. Specimen shrinkage due to the histological

treatments in the fibrous structure studies can be quantified according to this. But the decrease in cross-sectional area towards the insertion is not questioned.

The decrease in tendon cross-sectional area coincides with a decrease in fiber cross-sectional area and an increase in the size of spaces between the fibers towards the insertion. The fiber number stays nearly constant. The morphological findings from the first study suggest that the reduced fiber sizes could be a result of a decreased level of fiber crimping in the distal tendon near the *Tuber calcanei*, which could be caused by the compression against it. Additionally, compression could in itself lead to the finding of smaller cross-sectional areas. Vidal et al. (2015) found the fibers near the *Tuber calcanei* to be densely packed. Their “unpacked fibers” correspond well to the lower fiber gray values, found in the mineralized fibrocartilage in the fibrous structure scans.

The fibers appeared to be flattened, the ratio of the diameters was quantified to 0.63 in the later study. The quantitative study did not suggest a significantly higher degree of flattening adjacent to the *Tuber calcanei* in spite of the compression exerted. To the knowledge of the author, the aspect ratio of fibers is not yet covered in the literature. But it is mechanically relevant for fiber-matrix interaction and has implications for the interaction of the fibrils within the fiber. Interestingly, the aspect ratios of single fibers and the complete tendon are in the same range.

Deformation of the fibrous structure

Strain was measured along fibers. The structural correlates of the higher strain within the distal tendon are as yet unknown. But it corresponds well with the decrease in cross-sectional area that is thought to lead to higher stress.

At the tissue level, the increase in helical angle towards the insertion predicts an increase in strain. According to the high angular deviations, fiber realignment could be a major deformation mechanism causing the strain. Findings by Lake et al. (2009) show that an increasing fiber orientation contributes to strain of the insertion in the toe and the linear region during tensile tests. Their finding implies that a significant part of the load is transferred by matrix shearing. The matrix between the fibers accordingly has to resist shear by a relevant shear stiffness. In the free tendon the contribution of fiber realignment to tissue strain is restricted to the toe region (Lake et al., 2009). As previously stated, the increase in helical angle supports a high shear stiffness of the matrix. The differential reserve lengths among tendon portions contradict it. The contradiction can be reconciled within a model in which shear stiffness increases towards the insertion.

As delineated above, the classic “stretching-brake model” of fibrocartilage (Knese & Biermann, 1958) suggested that fibers curve around chondrons or even form a network around them, so that the chondrons are compressed between the fibers when a tensile load is applied. Even in recent models of fibrocartilage biomechanics, a compression of the matrix can only occur when fibers either exhibit a curvature or transversal connections that pull them together upon application of shear. Among the fiber courses of the Achilles tendon enthesis in mice, fiber curvature is primarily found in the form of helices and near the insertion. According to the prevailing poroelastic models of tendon and fibrocartilage (Wren et al., 2000; Ahmadzadeh et al., 2015), the matrix resists this compression by pressurization of the liquid phase and swelling pressure due to the negatively charged glycosaminoglycans. The time-dependent response of the matrix to the pressurization of the liquid depends on the permeability of the matrix. Permeability additionally decreases with compression.

The load cases of the proximal tendon and the distal tendon differ. The proximal tendon transfers a tensile load, while the distal tendon is additionally compressed against the *Tuber calcanei*. In the distal tendon, the volume losses are much higher than in the proximal tendon for this reason. Previous studies also found a higher permeability of the tendon near the insertion (Connizzo & Grodzinsky, 2017; 2018). The findings of the deformation study do not contradict this notion. Compression and permeability are also expected to interact with regard to their effect on the volume losses. The structural study showed that the spaces between the fibers are larger near the insertion. Such spaces correspond well to the finding of a higher permeability for liquid and to the idea that it could be caused by the collagen morphology (Connizzo & Grodzinsky, 2017; 2018). But the relevance of aggrecan content should not be neglected. Rigozzi et al. (2009) showed that glycosaminoglycan digestion leads to a decrease in modulus in the distal tendon.

The volume losses in the proximal tendon are still high for a tissue that is just compressed due to its helical structure. They support the idea that even tendon tissue that has not undergone fibrocartilaginous metaplasia is poroelastic (Ahmadzadeh et al., 2015). The observed accumulation of liquid in the bursa after load application supports the idea that liquid flow is important in the mechanical function of the enthesis. In future studies, dissection protocols and imaging intervals could be adapted in a way that enables exact measurement of the liquid exchange among the connective tissues and *bursae* of the ankle.

Reinforcement of the distal tendon

The decrease in cross-sectional area indicates that tensile stress should be increased towards the insertion. In the region with the smallest cross-sectional area, small curvature radii of the fibers were found. Low curvature radii lead to high levels of compressive stress between the fibers and the neighboring matrix (Giori et al., 1993). Accordingly, a high equivalent stress is expected to occur close to the insertion. This lends significance to the question how this region is reinforced if not in terms of structure. Based on a comment by a reviewer in the peer-review process of the fiber tracking study, the following mechanism is proposed.

The tensile strength of collagen fibrils depends on their water content (Sherman et al., 2015). Dehydration leads to a higher strength because more cross-links can be established among molecules. Liquid is pressed out of these tissues due to the compression in the curved tendon region. Glycosaminoglycans are bound in the tissue by the interactions with collagen (Vidal et al., 2015) and are kept in place during compression. They locally attract the remaining water and cause a dehydration of the neighboring fibrils. The previous description is a rough simplification. Of course, the short time intervals of dynamic loading and time-dependent liquid flows would have to be considered in a model. Nevertheless, there might be a level of compression that adds to the strength of the tissue. At higher levels the increase in equivalent stress is expected to lead to failure.

Mechanisms for homogenization of stress across the tendon

Based on the synopsis of structural findings and deformation behavior, the hypothesized mechanisms for stress homogenization across the tendon can be reexamined.

Higher reserve lengths were found in the superficial than in the deep tendon. But higher reserve lengths in the deep tendon would be required to compensate the lower initial length of the deep tendon. At the same time compression of the fibrocartilages is expected to lead to a relative release of tension within the superficial fibers. The reserve lengths were found at angles between the tendon and the *Calcaneus* axis near 90°. This is the lower end of the angular range found in locomotion (unpublished observation in X-ray videos). Increases in insertion angle would rather lead to further stretching of the deep fibers. Consequently, a contribution of reserve lengths to a homogeneous distribution of stress is not supported by the findings from the fibrous structure specimens. These notions require a reexamination in complete muscle-tendon units.

Helical fiber courses were found and they can clearly contribute to a homogenization of stress across the tendon. The poroelasticity of tendon tissue adds to this effect. The extent of the contribution might be restricted by the relatively straight fiber courses in the center of the tendon.

The branching rate of the fibers is too low to make significant contributions to the shear stiffness of the tissue except for small regions in the sesamoid fibrocartilage. But the combined finding of increasing helical angles and differential reserve lengths among tendon portions suggests that the matrix between the fibers could exhibit a higher shear stiffness in the insertion. Matrix shearing could therefore contribute to a homogenization of stress in the enthesis.

In such a model tendon portions could slide relative to one another far from the insertion. This is a prerequisite for stress homogenization by differential contraction of the connected muscles or motor-units.

The combination of tissue poroelasticity, liquid incompressibility and fiber curvature near the transition to mineralized fibrocartilage (Connizzo & Grodzinsky, 2017; 2018) could lead to a time-dependent homogenization of stress by local compensation of differential pressure in the liquid phase. Such behavior depends on the permeability of the tissue (Wren et al., 2000).

In conclusion, the helical arrangement of fibers is clearly supported as a homogenization mechanism. Matrix shearing, differential contraction of muscle portions and a combination of fiber curvature and poroelasticity could as well contribute. But parts of the structural and mechanical requirements for the function of these mechanisms are as yet unresolved. According to the tendon structure, differential reserve lengths cannot contribute to stress homogenization. Importantly, the helical arrangement of fibers and differential contraction of muscular portions are robust with regard to differences in initial length, changes in the insertion angle and time-dependent emergence of differential lengths.

Soft-hard transition

An important initial hypothesis was that fibrocartilage could differ from many engineering materials with regard to its transversal contraction. The structural prerequisites for a pressurization of the contained liquid under a tensile load are fulfilled near the insertion with bone. Fibers follow a curved course through the fibrocartilage matrix. Accordingly, the matrix is compressed and the contained liquid phase might be hindered from evading by the small pore spaces within the tissue and the adjacent mineralization front. The pressure in the liquid could therefore prevent the

transversal contraction of the fibrocartilage near the insertion over short load intervals and prevent stress singularities at the hard tissue interface. But the tomographies of the tissue under load had to be recorded after a relaxation time. At that point, (1) a pronounced transversal contraction and change in tissue volume was seen near the insertion, and (2) fibers experienced localized bending with low curvature radii. Both phenomena are thought to cause additional stress. Real-time radiographic series showed that decreases in volume and in the angles at the insertion occur nearly at the rate of load application. However, the loading rates were far below *in vivo* loading rates during locomotion. Thus, the hypothesis of a mechanism for prevention of transition stress based on liquid pressure can only be maintained for dynamic loads.

This finding has important physiological and clinical implications. The enthesis is thought to be less robust under sustained loads than under dynamic loads. In cyclic loading the strength of the enthesis is expected to decrease if the time under load is longer than the time for recovery of the lost liquid content due to the poroelasticity.

Evaluation of the approach

Analogies with hard-soft transitions in engineering raised the following question: Which structures and mechanisms contribute to a homogeneous distribution of stress along and across the transition between tendon and bone under physiological loads?

The problem of soft-hard transitions can be described easily in homogeneous, isotropic materials. But tendon, bone and the enthesial fibrocartilages are hierarchical with regard to structure and biomechanics. The author therefore found himself amid an ongoing discourse about the multiscale mechanics of tendon and fibrocartilage.

Three-dimensional imaging was used to explore the fibrous tissue structure at the Achilles tendon enthesis. Hypotheses with regard to the biomechanical functioning of the insertion as a soft-hard transition were developed based on geometrical and mechanical considerations, as well as the literature on the biomechanics of tendon and fibrocartilage. These hypotheses were checked by a combination of imaging and a mechanical test. A part of the hypotheses could be tested in these tests. However, imaging duration was shown to be more critical than initially expected. Therefore, a part of the questions has to be answered by future tests using techniques that have just become ready for application.

The accessibility of the Achilles tendon to dissection and imaging, as well as its size in mice contributed significantly to the level of detail and definition that was achieved in the imaging. With regard to structure, a fiber-centric approach was taken based on the simplistic idea that the fiber courses as such facilitate an understanding of the mechanics. But the mechanical state and properties of a fiber depend on the comprised hierarchical levels. The fibers are heterogeneous. The examination of the fibrous structure contributed a large part to the biomechanical models and the understanding of the Achilles tendon function in spite of this uncertainty.

Many explanations provided by this project relate to the concept of poroelasticity. The project could also be framed as an application of this concept to the tendon-bone insertion. But the relation of poroelasticity to the measurable structure of fibrocartilage needs to be elaborated to substantiate the suggested models and allow testing of the formulated ideas.

Perspectives

Future studies could expand this project in several directions. Some aspects of the enthesis structure and composition are challenging from an engineering perspective. Their function could be explored within biomimetic constructs. (1) In the enthesis, fibers and proteoglycans are connected. Upon compression, water is pressed out, but is drawn in again due to the polarity of the glycosaminoglycan chains. This composite seems to be especially efficient in a curved configuration, in which tension along the fibers and compression are superimposed. This function could be modeled in terms of a curved composite of fibers and hydrogels, that are bound to the fibers. (2) The helical arrangement of the tendon with a higher helical angle of fibers in the margins and higher orientation in the center could lead to a successive recruitment of fibers. The effect of differential fiber elasticity on the recruitment and stress distribution could be tested. (3) Eventually, the combination of the described hydrated composite with the helical arrangement could be evaluated with regard to stress homogenization.

The fiber tracks facilitate simulations of the mechanobiology and biomechanics of the Achilles tendon enthesis in mice. They could be further refined by a more elaborate examination of branching and validated using a different set of methods for staining, imaging and tracking. The workflow for the analysis of the fibrous structure of connective tissues enables examinations over the complete animal tree. But it is restricted with regard to specimen size. Complete muscle-tendon units in small animals are an ideal structure for a future study using this workflow – and would be a consequent research object based on this study.

To better understand enthesis structure, the testing of the formulated hypotheses using deformation experiments has to be pursued. Most importantly, the combination with radiographic series will enable the visualization of the tissue deformation at physiological loading rates. Shorter tomography times, lower radiation doses, smaller force intervals and a higher image quality are technically feasible and will facilitate tendon-wide automated pattern tracking and an analysis of the fiber orientations to examine the micromechanics leading to the macroscopic tissue response.

The project followed the long-term goal of collecting data fundamental for structurally-informed multiscale modeling of enthesis biomechanics. Going beyond this project the studies presented here could add together as follows: Using the three-dimensional spatial reference system from the first publication, fiber tracks from the second publication could be enriched with data on the distribution of matrix and fiber properties to create a multiscale model of the Achilles tendon enthesis in mice. Such a model could be used to simulate deformation under load – and evaluated by a 3D deformation study that measures local strain within the tissue.

4 Summary

At many tendon-bone insertions the tendon fibers pass through unmineralized and mineralized fibrocartilage before they dissociate at the interface with bone. The fibrocartilages are thought to mediate between the different mechanical behaviors of tendon and bone. The aims of this project are (1) to understand which aspects of the micromechanics of unmineralized fibrocartilage contribute to a homogeneous distribution of stress along the transition, and (2) to identify mechanisms within tendon and fibrocartilage that homogenize stress across the tendon.

Possible phenomena that could lead to stress singularities at the interface were deduced from an analogy between tendon-bone insertions and hard-soft transitions in engineering, such as terminations of polymer ropes at rigid frameworks. A mechanical model that explains how fibrocartilage could mitigate stress at the transition was derived from the literature. Five hypothetical mechanisms for stress homogenization were formulated following geometric and mechanical considerations: fiber interaction in helical arrangements, differential contraction of muscle portions, fiber curvature leading to interaction with the liquid phase of the matrix, shear transfer between fibers and differential reserve lengths in the relaxed state.

In the first part of the project the 3D fibrous structure of Achilles tendon entheses in mice is analyzed. To this end a workflow for connective tissue imaging, fiber tracking and fiber analysis is developed. The fibrous structure is compared to the structural prerequisites for the candidate mechanisms. The fibers are shown to follow helical courses with an increasing helical angle towards the insertion. They exhibit low levels of branching. Deep fibers inserting at the protrusion exhibit lower reserve lengths than superficial fibers. The fibers of the protrusion seem to correspond to a subtendon of other muscle bellies than the superficial fibers. In the distal tendon the fibers are curved towards the interface with bone.

Correspondingly, stress is homogenized due to (1) the interaction of the fibers in helical arrangements. (2) A correspondence of deep and superficial fibers to different muscle bellies enables stress homogenization due to differential muscle contraction. (3) Fibers that curve within the enthesial fibrocartilage are likely to exert compression on the neighboring matrix. Differential stress could therefore be compensated by local flow of interstitial liquid. (4) The increase in the fiber helical angle along the tendon is probably maintained by shear stiffness of the matrix. But it

does not seem to result from fiber branching. The reserve lengths of the fibers are distributed in a way that makes contributions to stress homogenization unlikely.

The second part of the project is a study of the 3D deformation of entheses in a tensile test. This study is carried out as well in murine Achilles tendon entheses to enable comparison with the structural examinations. The curvature of the distal tendon around the *Tuber calcanei* leads to a different loading of this region as compared to the proximal tendon. The mechanical behavior of these regions is compared with regard to stress, strain and volume losses. An emphasis is put on the deformation behavior at the interface with the hard tissue. It was examined with regard to deformation phenomena that could lead to local stress.

A tensile testing device is constructed in order to apply a tensile load to the enthesis that corresponds to the loading in locomotion with regard to angle and force level. The tensile test is mounted in a synchrotron beamline for deformation imaging. Therefore, the load case has to be quasi-static. Higher strains are found along fibers of the distal tendon. The structural basis of the compliance within fibers is as yet unclear. Higher volume losses in the distal region can be explained by the compression against the *Tuber calcanei*. Possible phenomena leading to stress maxima occur near the insertion. Hypothesized mechanisms for mitigation of stress maxima near the insertion cannot be applied if the fibrocartilage is subjected to sustained loads.

Future deformation studies have to show whether the hypothesized fibrocartilage behavior applies in the dynamic load case and whether there are further mechanisms that stabilize the transition under static loads. It should also examine the contributions of the candidate mechanisms to stress homogenization across the tendon. Critical parameters for deformation tests with higher temporal and spatial resolutions are deduced.

5 Zusammenfassung

An vielen Sehnenansätzen durchqueren die Sehnenfasern einen unmineralisierten und einen mineralisierten Faserknorpel bevor sie sich an der Knochenoberfläche in Fibrillen auflösen. Die Faserknorpel werden als Gewebe interpretiert, das zwischen den verschiedenen Materialeigenschaften von Knochen und Sehne vermittelt. Die Ziele dieses Projekts sind (1) zu verstehen welche Aspekte der Mikromechanik von Faserknorpel zu einer homogenen Spannungsverteilung entlang dieses Übergangs beitragen, und (2) Mechanismen zu identifizieren, die die Spannung gleichmäßig in Querschnitten von Sehne und Faserknorpel verteilen.

Phänomene, die zu Spannungsmaxima am Übergang zum Knochen beitragen können, werden aus dem Vergleich mit Hart-Weich-Übergängen in der Technik abgeleitet, zum Beispiel von Endanbindungen von Kunststoffseilen an starre Tragwerke. Ein mechanisches Modell, das beschreibt, wie Faserknorpel Spannungen am Übergang abmildern könnte, wird aus der Literatur hergeleitet. Die folgenden fünf Mechanismen, die zu einer gleichmäßigen Spannungsverteilung über den Querschnitt beitragen könnten, werden aufgrund geometrischer und mechanischer Überlegungen postuliert: Faserinteraktion aufgrund helikaler Verläufe, unterschiedliche Kontraktion der verbundenen Muskelportionen, Druckausgleich über die flüssige Phase an gekrümmten Fasern, Schubübertragung zwischen Fasern und angepasste Dehnungsreserven.

Das erste Teilprojekt ist eine Analyse der 3D Faserstruktur am Achillessehnenansatz von Mäusen. Dazu wird ein Arbeitsablauf mit folgenden Schritten entwickelt: Visualisierung des Bindegewebes, Faserverfolgung und Faseranalyse. Es wird überprüft, ob die Faserstruktur die strukturellen Voraussetzungen für die formulierten Mechanismen erfüllt. Die Fasern folgen helikalen Verläufen mit einem zunehmenden Winkel zur Sehnenachse in Richtung des Ansatzes. Sie weisen geringe Verzweigungsraten auf. Fasern der tiefen Sehne setzen an einem Knochenvorsprung an und weisen geringere Dehnungsreserven auf als oberflächliche Fasern. Sie scheinen der Teilsehne anderer Muskelbäuche zu entsprechen als die oberflächlichen Fasern. In der distalen Sehne sind die Faserverläufe zur Knochenoberfläche hin gekrümmt.

Die Spannung wird demnach aufgrund (1) der Faserinteraktion in helikalen Verläufen gleichmäßiger verteilt. (2) Die Verbindung tiefer und oberflächlicher Fasern mit unterschiedlichen Muskelbäuchen ermöglicht einen Spannungsausgleich durch angepasste Muskelkontraktion. (3) Gekrümmte Faserverläufe bewirken bei Kraftübertragung eine Kompression der benachbarten

Matrix. Spannungsunterschiede können daher durch lokale Bewegungen der interstitiellen Flüssigkeit ausgeglichen werden. (4) Der zunehmende Helixwinkel in Richtung des Ansatzes wird vermutlich durch Schersteifigkeit der Matrix aufrechterhalten. Die Schersteifigkeit basiert allerdings nicht auf Faserverzweigungen. Die Dehnungsreserven sind so verteilt, dass ein Beitrag zu einer gleichmäßigen Spannungsverteilung unwahrscheinlich ist.

Im zweiten Teilprojekt wird die dreidimensionale Verformung von Enthesen im Zugversuch untersucht. Auch dabei ist der Untersuchungsgegenstand der Achillessehnenansatz bei Mäusen, so dass die Ergebnisse mit den strukturellen Befunden verglichen werden können. Aus der Krümmung der distalen Sehne am *Tuber calcanei* kann abgeleitet werden, dass diese Region und die freie proximale Sehne sich hinsichtlich der Belastung unterscheiden. Daher wird das mechanische Verhalten dieser Sehnenteile hinsichtlich der Spannung, der Dehnung und des Volumenverlustes verglichen. Ein weiterer Schwerpunkt ist die Untersuchung der Verformung am Übergang zum Knochen. Sie wurde auf Verformungsmuster überprüft, die zu lokalen Spannungskonzentrationen führen können.

Der Zugversuchsapparat für diese Studie ist so gestaltet, dass die Zugkraft der Belastung während der Fortbewegung hinsichtlich der Richtung und des Betrags entspricht. Er wird in die Messstrecke eines Synchrotronstrahlengangs eingebaut, um die dreidimensionale Verformung aufzunehmen. Dazu muss ein quasistatischer Lastfall erzielt werden. Höhere Dehnungen in Faserrichtung werden in der distalen Sehne gefunden. Der strukturelle Grund für die höhere Nachgiebigkeit ist noch unbekannt. Höhere Volumenverluste in diesem Teil der Sehne sind vermutlich auf den Druck zwischen der Sehne und dem *Tuber calcanei* zurückzuführen. Am Knochenübergang verformt sich die Sehne so, dass Spannungsmaxima wahrscheinlich auftreten. Demnach funktioniert der Faserknorpel zumindest unter anhaltenden Lasten nicht so wie angenommen.

Weitere Verformungsstudien sind nötig, um zu überprüfen, ob der vorgeschlagene Mechanismus unter dynamischen Lasten zur Spannungsvermeidung beitragen kann und ob es andere Mechanismen gibt, die den Übergang gegenüber anhaltenden Lasten verstärken. Auch der Anteil der verschiedenen Mechanismen an einer gleichmäßigen Spannungsverteilung über die Sehne könnte dabei untersucht werden. Durch welche Einstellungen Verformungsversuche mit höherer zeitlicher und räumlicher Auflösung erreicht werden können wird dargestellt.

6 References

Ahmadzadeh H, Freedman BR, Connizzo BK, et al. (2015) Micromechanical poroelastic finite element and shear-lag models of tendon predict large strain dependent Poisson's ratios and fluid expulsion under tensile loading. *Acta Biomaterialia* **22**, 83–91.

Alexander RM (2002) Tendon elasticity and muscle function. *Comparative Biochemistry and Physiology Part A: Molecular & Integrative Physiology* **133**, 1001–1011.

Ashton-Miller JA, He Y, Kadhiresan VA, et al. (1992) An apparatus to measure in vivo biomechanical behavior of dorsi- and plantarflexors of mouse ankle. *Journal of Applied Physiology* **72**, 1205–1211.

Bailly L, Cochereau T, Orgéas L, et al. (2018) 3D multiscale imaging of human vocal folds using synchrotron X-ray microtomography in phase retrieval mode. *Sci Rep* **8**, 14003.

Balijepalli RG, Begley MR, Fleck NA, et al. (2016) Numerical simulation of the edge stress singularity and the adhesion strength for compliant mushroom fibrils adhered to rigid substrates. *International Journal of Solids and Structures* **85–86**, 160–171.

Balint R, Lowe T, Shearer T (2016) Optimal Contrast Agent Staining of Ligaments and Tendons for X-Ray Computed Tomography. *PLoS ONE* **11**, e0153552.

Bannerman A, Paxton JZ, Grover LM (2014) Imaging the hard/soft tissue interface. *Biotechnology Letters* **36**, 403–415.

Barfred T (1973) Achilles tendon rupture: aetiology and pathogenesis of subcutaneous rupture assessed on the basis of the literature and rupture experiments on rats. *Acta Orthopaedica Scandinavica* **44**, 1–126.

Benjamin M, Evans EJ, Copp L (1986) The histology of tendon attachments to bone in man. *Journal of anatomy* **149**, 89–100.

Benjamin M, Kumai T, Milz S, et al. (2002) The skeletal attachment of tendons—tendon 'entheses.' *Comparative Biochemistry and Physiology Part A: Molecular & Integrative Physiology* **133**, 931–945.

Benjamin M, McGonagle D (2001) The anatomical basis for disease localisation in seronegative spondyloarthropathy at entheses and related sites. *Journal of Anatomy* **199**, 503–526.

Benjamin M, Ralphs JR (1998) Fibrocartilage in tendons and ligaments—an adaptation to compressive load. *Journal of anatomy* **193**, 481–494.

Benjamin M, Ralphs JR (2000) Entheses – the bony attachments of tendons and ligaments. *Italian journal of anatomy and embryology* **106**, 151–157.

Benjamin M, Ralphs JR (2004) Biology of fibrocartilage cells. *Int Rev Cytol* **233**, 1–45.

Benjamin M, Toumi H, Ralphs JR, et al. (2006) Where tendons and ligaments meet bone: attachment sites ('entheses') in relation to exercise and/or mechanical load. *Journal of Anatomy* **208**, 471–490.

Bey MJ, Song HK, Wehrli FW, et al. (2002) Intratendinous strain fields of the intact supraspinatus tendon: the effect of glenohumeral joint position and tendon region. *J Orthop Res* **20**, 869–874.

Birch HL, Thorpe CT, Rumian AP (2013) Specialisation of extracellular matrix for function in tendons and ligaments. *Muscles, Ligaments and Tendons Journal* **3**, 12–22.

Birk DE, Southern JF, Zycband EI, et al. (1989) Collagen fibril bundles: a branching assembly unit in tendon morphogenesis. *Development* **107**, 437–443.

Birk DE, Zycband EI, Woodruff S, et al. (1997) Collagen fibrillogenesis in situ: Fibril segments become long fibrils as the developing tendon matures. *Developmental Dynamics* **208**, 291–298.

Bogy DB (1968) Edge-Bonded Dissimilar Orthogonal Elastic Wedges Under Normal and Shear Loading. *Journal of Applied Mechanics* **35**, 460–466.

Butler D, Grood E, Noyes F, et al. (1978) Biomechanics of ligaments and tendons. *Exercise and Sport Sciences Reviews* **6**, 125–181.

Buytaert J, Goyens J, De Greef D, et al. (2014) Volume Shrinkage of Bone, Brain and Muscle Tissue in Sample Preparation for Micro-CT and Light Sheet Fluorescence Microscopy (LSFM). *Microscopy and Microanalysis* **20**, 1208–1217.

Canoso J (1998) The premiere enthesis. *Journal of rheumatology* **25**, 1254–1256.

Canoso JJ, Liu N, Traill MR, et al. (1988) Physiology of the retrocalcaneal bursa. *Annals of the rheumatic diseases* **47**, 910–912.

Carter DR (1987) Mechanical loading history and skeletal biology. *Journal of Biomechanics* **20**, 1095–1109.

Carter DR, Beaupre GS, Giori NJ, et al. (1998) Mechanobiology of Skeletal Regeneration. *Clinical orthopaedics and related research* **355**, 41–55.

Chandrasekaran S, Pankow M, Peters K, et al. (2017) Composition and structure of porcine digital flexor tendon-bone insertion tissues. *J Biomed Mater Res, Part A* **105**, 3050–3058.

Clark J, Stechschulte DJJ (1998) The interface between bone and tendon at an insertion site: a study of the quadriceps tendon insertion. *J Anat* **192**, 605–616.

Connizzo BK, Adams SM, Adams TH, et al. (2016) Multiscale regression modeling in mouse supraspinatus tendons reveals that dynamic processes act as mediators in structure–function relationships. *Journal of Biomechanics* **49**, 1649–1657.

Connizzo BK, Grodzinsky AJ (2017) Tendon exhibits complex poroelastic behavior at the nanoscale as revealed by high-frequency AFM-based rheology. *Journal of Biomechanics* **54**, 11–18.

Connizzo BK, Grodzinsky AJ (2018) Multiscale Poroviscoelastic Compressive Properties of Mouse Supraspinatus Tendons Are Altered in Young and Aged Mice. *Journal of Biomechanical Engineering* **140**, 051002.

Connizzo BK, Sarver JJ, Han L, et al. (2014) In situ fibril stretch and sliding is location-dependent in mouse supraspinatus tendons. *Journal of Biomechanics* **47**, 3794–3798.

Cooper RR, Misol S (1970) Tendon and ligament insertion: A light and electron microscopic study. *The Journal of Bone & Joint Surgery* **52**, 1–170.

Correia M, Deffieux T, Chatelin S, et al. (2018) 3D elastic tensor imaging in weakly transversely isotropic soft tissues. *Phys Med Biol* **63**, 155005.

Cummins EJ, Anson BJ, Carr WB, et al. (1946) The structure of the calcaneal tendon (of Achilles) in relation to orthopedic surgery, with additional observations on the plantaris muscle. *Surgery, gynecology & obstetrics* **83**, 107–116.

Dai C, Guo L, Yang L, et al. (2014) Regional fibrocartilage variations in human anterior cruciate ligament tibial insertion: a histological three-dimensional reconstruction. *Connect Tissue Res* **56**, 18–24.

Denk W, Horstmann H (2004) Serial Block-Face Scanning Electron Microscopy to Reconstruct Three-Dimensional Tissue Nanostructure. *PLoS Biology* **2**, e329.

Depalle B, Qin Z, Shefelbine SJ, et al. (2015) Influence of cross-link structure, density and mechanical properties in the mesoscale deformation mechanisms of collagen fibrils. *Journal of the Mechanical Behavior of Biomedical Materials* **52**, 1–13.

Deymier AC, An Y, Boyle JJ, et al. (2017) Micro-mechanical properties of the tendon-to-bone attachment. *Acta Biomaterialia* **65**, 25–35.

Deymier-Black AC, Pasteris JD, Genin GM, et al. (2015) Allometry of the Tendon Enthesis: Mechanisms of Load Transfer Between Tendon and Bone. *Journal of Biomechanical Engineering* **137**, 111005 (8).

Diamant J, Keller A, Baer E, et al. (1972) Collagen; Ultrastructure and Its Relation to Mechanical Properties as a Function of Ageing. *Proceedings of the Royal Society B: Biological Sciences* **180**, 293–315.

Dickinson E, Stark H, Kupczik K (2018) Non-Destructive Determination of Muscle Architectural Variables Through the Use of DiceCT. *Anat Rec* **301**, 363–377.

Disney CM, Eckersley A, McConnell JC, et al. (2019) Synchrotron tomography of intervertebral disc deformation quantified by digital volume correlation reveals microstructural influence on strain patterns. *Acta Biomaterialia* **92**, 290–304.

Disney CM, Lee PD, Hoyland JA, et al. (2018) A review of techniques for visualising soft tissue microstructure deformation and quantifying strain *Ex Vivo*. *Journal of Microscopy* **272**, 165–179.

Disney CM, Madi K, Bodey AJ, et al. (2017) Visualising the 3D microstructure of stained and native intervertebral discs using X-ray microtomography. *Sci Rep* **7**, 16279.

Djukic K, Milovanovic P, Hahn M, et al. (2015) Bone microarchitecture at muscle attachment sites: The relationship between macroscopic scores of entheses and their cortical and trabecular microstructural design. *American Journal of Physical Anthropology* **157**, 81–93.

Dolgo-Saburoff B (1929) Über Ursprung und Insertion der Skelettmuskeln. *Anat Anz* **68**, 80–87.

Dörfl J (1980) Migration of tendinous insertions. I. Cause and mechanism. *Journal of anatomy* **131**, 179.

Edama M, Kubo M, Onishi H, et al. (2015) The twisted structure of the human Achilles tendon: Classification by degree of twist. *Scand J Med Sci Sports* **25**, e497–e503.

Edama M, Kubo M, Onishi H, et al. (2016) Structure of the Achilles tendon at the insertion on the calcaneal tuberosity. *Journal of Anatomy* **229**, 610–614.

Finni T, Bernabei M, Baan GC, et al. (2018) Non-uniform displacement and strain between the soleus and gastrocnemius subtendons of rat Achilles tendon. *Scand J Med Sci Sports* **28**, 1009–1017.

Fischer MS, Schilling N, Schmidt M, et al. (2002) Basic limb kinematics of small therian mammals. *Journal of Experimental Biology* **205**, 1315–1338.

Franchi M, Fini M, Quaranta M, et al. (2007) Crimp morphology in relaxed and stretched rat Achilles tendon. *Journal of Anatomy* **210**, 1–7.

Franchi M, Ottani V, Stagni R, et al. (2010) Tendon and ligament fibrillar crimps give rise to left-handed helices of collagen fibrils in both planar and helical crimps. *Journal of Anatomy* **216**, 301–309.

Franchi M, Raspanti M, Dell'Orbo C, et al. (2008) Different Crimp Patterns in Collagen Fibrils Relate to the Subfibrillar Arrangement. *Connective Tissue Research* **49**, 85–91.

Fratzl P, Misof K, Zizak I, et al. (1998) Fibrillar Structure and Mechanical Properties of Collagen. *Journal of Structural Biology* **122**, 119–122.

Frizziero A, Fini M, Salamanna F, et al. (2011) Effect of training and sudden detraining on the patellar tendon and its enthesis in rats. *BMC musculoskeletal disorders* **12**, 20.

Galatz L, Rothermich S, VanderPloeg K, et al. (2007) Development of the supraspinatus tendon-to-bone insertion: Localized expression of extracellular matrix and growth factor genes. *Journal of Orthopaedic Research* **25**, 1621–1628.

Gao J, Messner K, Ralphs JR, et al. (1996) An immunohistochemical study of enthesis development in the medial collateral ligament of the rat knee joint. *Anatomy & Embryology* **194**, 399–406.

Gelse K, Pöschl E, Aigner T (2003) Collagens—structure, function, and biosynthesis. *Advanced Drug Delivery Reviews* **55**, 1531–1546.

Genin GM, Thomopoulos S (2017) The tendon-to-bone attachment: Unification through disarray. *Nature Materials* **16**, 607–608.

Giori NJ, Beaupré GS, Carter DR (1993) Cellular shape and pressure may mediate mechanical control of tissue composition in tendons. *Journal of Orthopaedic Research* **11**, 581–591.

Gradl R, Dierolf M, Hehn L, et al. (2017) Propagation-based Phase-Contrast X-ray Imaging at a Compact Light Source. *Scientific Reports* **7**, 4908.

Greving I, Wilde F, Ogurreck M, et al. (2014) P05 imaging beamline at PETRA III: first results. In S. R. Stock, ed. SPIE Optical Engineering + Applications. San Diego, California, United States, 92120O.

Gupta HS, Seto J, Krauss S, et al. (2010) In situ multi-level analysis of viscoelastic deformation mechanisms in tendon collagen. *Journal of Structural Biology* **169**, 183–191.

Han M, Larson PE, Liu J, et al. (2014) Depiction of Achilles Tendon Microstructure In Vivo Using High-Resolution 3-Dimensional Ultrashort Echo-Time Magnetic Resonance Imaging at 7 T. *Investigative radiology* **49**, 339–345.

Han WM, Heo S-J, Driscoll TP, et al. (2016) Microstructural heterogeneity directs micromechanics and mechanobiology in native and engineered fibrocartilage. *Nature Mater* **15**, 477–484.

Handsfield GG, Slane LC, Screen HRC (2016) Nomenclature of the tendon hierarchy: An overview of inconsistent terminology and a proposed size-based naming scheme with terminology for multi-muscle tendons. *Journal of Biomechanics* **49**, 3122–3124.

Hipp A, Herzen J, Hammel J, et al. (2016) Single-grating interferometer for high-resolution phase-contrast imaging at synchrotron radiation sources. In *Developments in X-Ray Tomography X*. International Society for Optics and Photonics, 996718.

Hipp AC (2017) *High-resolution grating-based phase contrast for synchrotron radiation sources*. Hamburg: Universität Hamburg.

Hipp AC, Moosmann J, Herzen J, et al. (2017) High-resolution grating interferometer for phase-contrast imaging at PETRA III. In B. Müller & G. Wang, eds. *Proc. SPIE 10391*. Developments in X-Ray Tomography XI. San Diego, California, United States: International Society for Optics and Photonics.

Ho SP, Kurylo MP, Fong TK, et al. (2010) The biomechanical characteristics of the bone-periodontal ligament-cementum complex. *Biomaterials* **31**, 6635–6646.

Holschemacher D, Streubel P, Michael, Markus (2016) Endverbindungen für dynamisch belastete textile Zugmittel. *Logistics Journal: Proceedings* **5**, 9.

Hoover EE, Squier JA (2013) Advances in multiphoton microscopy technology. *Nature photonics* **7**, 93–101.

Jacques P, Lambrecht S, Verheugen E, et al. (2014) Proof of concept: enthesitis and new bone formation in spondyloarthritis are driven by mechanical strain and stromal cells. *Ann Rheum Dis* **73**, 437–445.

Jeffery NS, Stephenson RS, Gallagher JA, et al. (2011) Micro-computed tomography with iodine staining resolves the arrangement of muscle fibres. *Journal of Biomechanics* **44**, 189–192.

Jensen PT, Lambertsen KL, Frich LH (2018) Assembly, maturation, and degradation of the supraspinatus enthesis. *J Shoulder Elbow Surg*.

Jozsa L, Kvist M, Balint BJ, et al. (1989) The role of recreational sport activity in Achilles tendon rupture A clinical, pathoanatomical, and sociological study of 292 cases. *The American Journal of Sports Medicine* **17**, 338–343.

Kalson NS, Malone PSC, Bradley RS, et al. (2012) Fibre bundles in the human extensor carpi ulnaris tendon are arranged in a spiral. *Journal of Hand Surgery (European Volume)* **37**, 550–554.

Kanazawa T, Gotoh M, Ohta K, et al. (2016) Three-dimensional ultrastructural analysis of development at the supraspinatus insertion by using focused ion beam/scanning electron microscope tomography in rats. *J Orthop Res* **34**, 969–976.

Kanazawa T, Gotoh M, Shiba N, et al. (2014) Novel characteristics of normal supraspinatus insertion in rats: an ultrastructural analysis using three-dimensional reconstruction using focused ion beam/scanning electron microscope tomography. *Muscles Ligaments Tendons J* **4**, 182–7.

Kanazawa T, Ohta K, Nakamura K-I, et al. (2016) Histomorphometric and ultrastructural analysis of the tendon-bone interface after rotator cuff repair in a rat model. *Sci Rep* **6**, 33800.

Ker R (2007) Mechanics of tendon, from an engineering perspective. *International Journal of Fatigue* **29**, 1001–1009.

Ker RF, Alexander RMcn, Bennett MB (1988) Why are mammalian tendons so thick? *Journal of Zoology* **216**, 309–324.

Kerckhofs G, Stegen S, Van Gastel N, et al. (2016) Novel non-invasive micro-CT contrast agent for quantitative virtual 3D histology of mineralized and soft skeletal tissues. In *Proceedings of IEEE International Symposium on Biomedical Imaging*.

Khoury BM, Bigelow EMR, Smith LM, et al. (2015) The use of nano-computed tomography to enhance musculoskeletal research. *Connective Tissue Research* **56**, 106–119.

Kiani C, Chen L, Wu YJ, et al. (2002) Structure and function of aggrecan. *Cell Res* **12**, 19–32.

Killian ML, Thomopoulos Stavros (2016) Scleraxis is required for the development of a functional tendon enthesis. *FASEB J* **30**, 301–311.

Kizilyaprak C, Daraspe J, Humbel BM (2014) Focused ion beam scanning electron microscopy in biology. *Journal of Microscopy* **254**, 109–114.

Klika V, Whiteley JP, Brown CP, et al. (2019) The combined impact of tissue heterogeneity and fixed charge for models of cartilage: the one-dimensional biphasic swelling model revisited. *Biomech Model Mechanobiol* **18**, 953–968.

Knese K-H, Biermann H (1958) Die Knochenbildung an Sehnen-und Bandansätzen im Bereich ursprünglich chondraler Apophysen. *Zeitschrift fuer Zellforschung und mikroskopische Anatomie* **49**, 142–187.

Kuntz LA, Rossetti L, Kunold E, et al. (2018) Biomarkers for tissue engineering of the tendon-bone interface. *PLOS ONE* **13**, e0189668.

Kupczik K, Stark H, Mundry R, et al. (2015) Reconstruction of muscle fascicle architecture from iodine-enhanced microCT images: A combined texture mapping and streamline approach. *Journal of Theoretical Biology* **382**, 34–43.

Lake SP, Miller KS, Elliott DM, et al. (2009) Effect of fiber distribution and realignment on the nonlinear and inhomogeneous mechanical properties of human supraspinatus tendon under longitudinal tensile loading. *Journal of Orthopaedic Research* **27**, 1596–1602.

Landis WJ, Hodgens KJ, Arena J, et al. (1996) Structural relations between collagen and mineral in bone as determined by high voltage electron microscopic tomography. *Microscopy research and technique* **33**, 192–202.

Lautner S, Lenz C, Hammel JU, et al. (2017) Using SRμCT to define water transport capacity in Picea abies. In B. Müller & G. Wang, eds. *Developments in X-Ray Tomography XI*. San Diego, United States: International Society for Optics and Photonics, 53.

Libanori R, Erb RM, Reiser A, et al. (2012) Stretchable heterogeneous composites with extreme mechanical gradients. *Nature Communications* **3**, 1265.

Liu J, Lin S, Liu X, et al. (2020) Fatigue-resistant adhesion of hydrogels. *Nat Commun* **11**, 1071.

Liu Y (2012) *The Mechanics of Bimaterial Attachment at the Tendon-to-Bone Insertion Site*. St. Louis, Missouri, USA: Washington University.

Liu Y, Thomopoulos S, Chen C, et al. (2014) Modelling the mechanics of partially mineralized collagen fibrils, fibres and tissue. *Journal of the Royal Society Interface* **11**, UNSP 20130835.

Liu YX, Thomopoulos S, Birman V, et al. (2012) Bi-material attachment through a compliant interfacial system at the tendon-to-bone insertion site. *Mechanics of Materials* **44**, 83–92.

Locke RC, Peloquin JM, Lemmon EA, et al. (2017) Strain Distribution of Intact Rat Rotator Cuff Tendon-to-Bone Attachments and Attachments With Defects. *Journal of biomechanical engineering* **139**, 111007.

Lu HH, Thomopoulos S (2013) Functional Attachment of Soft Tissues to Bone: Development, Healing, and Tissue Engineering M. L. Yarmush, ed. *Annual Review of Biomedical Engineering, Vol 15* **15**, 201–226.

Luetkemeyer CM, Cai L, Neu CP, et al. (2018) Full-volume displacement mapping of anterior cruciate ligament bundles with dualMRI. *Extreme Mechanics Letters* **19**, 7–14.

Malaviya P, Bultler DL, Boivin GP, et al. (2000) An *in vivo* model for load-modulated remodeling in the rabbit flexor tendon. *J Orthop Res* **18**, 116–125.

Mallett KF, Arruda EM (2017) Digital image correlation-aided mechanical characterization of the anteromedial and posterolateral bundles of the anterior cruciate ligament. *Acta biomaterialia* **56**, 44–57.

Matyas JR, Anton MG, Shrive NG, et al. (1995) Stress governs tissue phenotype at the femoral insertion of the rabbit MCL. *Journal of Biomechanics* **28**, 147–157.

Mayo SC, Stevenson AW, Wilkins SW (2012) In-Line Phase-Contrast X-ray Imaging and Tomography for Materials Science. *Materials (Basel)* **5**, 937–965.

McNeilly C, Banes A, Benjamin M, et al. (1996) Tendon cells in vivo form a three dimensional network of cell processes linked by gap junctions. *Journal of anatomy* **189**, 593.

Mente PL, Lewis JL (1994) Elastic modulus of calcified cartilage is an order of magnitude less than that of subchondral bone. *Journal of Orthopaedic Research* **12**, 637–647.

Miller KS, Connizzo BK, Feeney E, et al. (2012) Examining Differences in Local Collagen Fiber Crimp Frequency Throughout Mechanical Testing in a Developmental Mouse Supraspinatus Tendon Model. *Journal of Biomechanical Engineering* **134**, 041004.

Miller KS, Connizzo BK, Soslowsky LJ (2012) Collagen Fiber Re-Alignment in a Neonatal Developmental Mouse Supraspinatus Tendon Model. *Annals of Biomedical Engineering* **40**, 1102–1110.

Miller KS, Edelstein L, Connizzo BK, et al. (2012) Effect of Preconditioning and Stress Relaxation on Local Collagen Fiber Re-Alignment: Inhomogeneous Properties of Rat Supraspinatus Tendon. *Journal of Biomechanical Engineering* **134**, 031007.

Milz S, Rufai A, Buettner A, et al. (2002) Three-dimensional reconstructions of the Achilles tendon insertion in man. *Journal of Anatomy* **200**, 145–152.

Mizutani R, Takeuchi A, Uesugi K, et al. (2010) Microtomographic Analysis of Neuronal Circuits of Human Brain. *Cerebral Cortex* **20**, 1739–1748.

Moosmann J, Wieland DCF, Zeller-Plumhoff B, et al. (2019) A load frame for in situ tomography at PETRA III. In B. Müller & G. Wang, eds. *Proc. SPIE 11113*. Developments

in X-Ray Tomography XII. San Diego, United States: International Society for Optics and Photonics, 41.

Morgan KS, Siu KKW, Paganin DM (2010) The projection approximation and edge contrast for x-ray propagation-based phase contrast imaging of a cylindrical edge. *Optics Express* **18**, 9865.

Mori S, Crain BJ, Chacko VP, et al. (1999) Three-dimensional tracking of axonal projections in the brain by magnetic resonance imaging. *Annals of Neurology* **45**, 265–269.

Munz D, Yang Y (1992) Stress singularities at the interface in bonded dissimilar materials under mechanical and thermal loading. *Journal of Applied Mechanics* **59**, 857–861.

Naveh GRS, Brumfeld V, Shahar R, et al. (2013) Tooth periodontal ligament: Direct 3D microCT visualization of the collagen network and how the network changes when the tooth is loaded. *Journal of Structural Biology* **181**, 108–115.

Nazarian A, Araiza Arroyo FJ, Rosso C, et al. (2011) Tensile properties of rat femoral bone as functions of bone volume fraction, apparent density and volumetric bone mineral density. *Journal of Biomechanics* **44**, 2482–2488.

Nia HT, Han L, Soltani Bozchalooi I, et al. (2015) Aggrecan Nanoscale Solid–Fluid Interactions Are a Primary Determinant of Cartilage Dynamic Mechanical Properties. *ACS Nano* **9**, 2614–2625.

Nierenberger M, Rémond Y, Ahzi S, et al. (2015) Assessing the three-dimensional collagen network in soft tissues using contrast agents and high resolution micro-CT: Application to porcine iliac veins. *Comptes Rendus Biologies* **338**, 425–433.

Nyakatura JA, Stark H (2015) Aberrant back muscle function correlates with intramuscular architecture of dorsovertebral muscles in two-toed sloths. *Mammalian Biology* **80**, 114–121.

Ohtani O (1987) Three-dimensional organization of the connective tissue fibers of the human pancreas: a scanning electron microscopic study of NaOH treated-tissues. *Arch Histol Jpn* **50**, 557–566.

Ohtani O, Ushiki T, Taguchi T, et al. (1988) Collagen fibrillar networks as skeletal frameworks: a demonstration by cell-maceration/scanning electron microscope method. *Archives of histology and cytology* **51**, 249–261.

Pauwels F (1960) Eine neue Theorie über den Einfluß mechanischer Reize auf die Differenzierung der Stützgewebe. *Zeitschrift für Anatomie und Entwicklungsgeschichte* **121**, 478–515.

Ploetz E (1938) Funktioneller Bau und funktionelle Anpassung der Gleitsehnen. *Zeitschrift für Orthopädie* **67**, 212–234.

Provenzano PP, Vanderby R (2006) Collagen fibril morphology and organization: Implications for force transmission in ligament and tendon. *Matrix Biology* **25**, 71–84.

Puxkandl R, Zizak I, Paris O, et al. (2002) Viscoelastic properties of collagen: synchrotron radiation investigations and structural model. *Philosophical Transactions of the Royal Society of London Series B: Biological Sciences* **357**, 191–197.

Quigley AS, Bancelin S, Deska-Gauthier D, et al. (2018) In tendons, differing physiological requirements lead to functionally distinct nanostructures. *Sci Rep* **8**, 4409.

Ralphs JR, Benjamin M, Waggett AD, et al. (1998) Regional differences in cell shape and gap junction expression in rat Achilles tendon: relation to fibrocartilage differentiation. *J Anat* **193**, 215–222.

Reese SP, Maas SA, Weiss JA (2010) Micromechanical models of helical superstructures in ligament and tendon fibers predict large Poisson's ratios. *Journal of Biomechanics* **43**, 1394–1400.

Reese TG, Weisskoff RM, Smith RN, et al. (1995) Imaging myocardial fiber architecture *in vivo* with magnetic resonance. *Magn Reson Med* **34**, 786–791.

Reeves ND, Cooper G (2017) Is human Achilles tendon deformation greater in regions where cross-sectional area is smaller? *The Journal of Experimental Biology* **220**, 1634–1642.

Rho JY, Ashman RB, Turner CH (1993) Young's modulus of trabecular and cortical bone material: Ultrasonic and microtensile measurements. *Journal of Biomechanics* **26**, 111–119.

Riemersma DJ, De Bruyn P (1986) Variations in cross-sectional area and composition of equine tendons with regard to their mechanical function. *Research in veterinary science* **41**, 7–13.

Riggin CN, Sarver JJ, Freedman BR, et al. (2014) Analysis of Collagen Organization in Mouse Achilles Tendon Using High-Frequency Ultrasound Imaging. *Journal of Biomechanical Engineering* **136**, 021029.

Rigozzi S, Muller R, Snedeker JG (2009) Local strain measurement reveals a varied regional dependence of tensile tendon mechanics on glycosaminoglycan content. *J Biomech* **42**, 1547–52.

Rigozzi S, Stemmer A, Müller R, et al. (2011) Mechanical response of individual collagen fibrils in loaded tendon as measured by atomic force microscopy. *Journal of Structural Biology* **176**, 9–15.

Rossetti L, Kuntz LA, Kunold E, et al. (2017) The microstructure and micromechanics of the tendon–bone insertion. *Nature Materials* **16**, 664–670.

Rufai A, Benjamin M, Ralphs J (1992) Development and ageing of phenotypically distinct fibrocartilages associated with the rat Achilles tendon. *Anatomy and embryology* **186**, 611–618.

Rufai A, Ralphs JR, Benjamin M (1995) Structure and histopathology of the insertional region of the human Achilles tendon. *Journal of orthopaedic research* **13**, 585–593.

Rufai A, Ralphs JR, Benjamin M (1996) Ultrastructure of fibrocartilages at the insertion of the rat Achilles tendon. *Journal of anatomy* **189**, 185.

Sanchez S, Dupret V, Tafforeau P, et al. (2013) 3D microstructural architecture of muscle attachments in extant and fossil vertebrates revealed by synchrotron microtomography. *PLoS One* **8**, e56992.

Sano H, Saijo Y, Kokubun S (2006) Non-mineralized fibrocartilage shows the lowest elastic modulus in the rabbit supraspinatus tendon insertion: Measurement with scanning acoustic microscopy. *Journal of Shoulder and Elbow Surgery* **15**, 743–749.

Sasaki N, Odajima S (1996) Elongation mechanism of collagen fibrils and force-strain relations of tendon at each level of structural hierarchy. *Journal of biomechanics* **29**, 1131–1136.

Schenk P, Siebert T, Hiepe P, et al. (2013) Determination of three-dimensional muscle architectures: validation of the DTI-based fiber tractography method by manual digitization. *Journal of Anatomy* **223**, 61–68.

Schneider H (1956) Zur Struktur der Sehnenansatzzonen. *Anatomy and Embryology* **119**, 431–456.

Schünke M (2014) *Funktionelle Anatomie: Topografie und Funktion des Bewegungssystems*, Stuttgart: Thieme.

Schwartz AG, Pasteris JD, Genin GM, et al. (2012) Mineral Distributions at the Developing Tendon Enthesis. *PLoS ONE* **7**, e48630.

Screen HRC (2008) Investigating load relaxation mechanics in tendon. *Journal of the Mechanical Behavior of Biomedical Materials* **1**, 51–58.

Screen HRC, Bader DL, Lee DA, et al. (2004) Local Strain Measurement within Tendon. *Strain* **40**, 157–163.

Screen HRC, Berk DE, Kadler KE, et al. (2015) Tendon Functional Extracellular Matrix. *J Orthop Res* **33**, 793–799.

Screen HRC, Toorani S, Shelton JC (2013) Microstructural stress relaxation mechanics in functionally different tendons. *Medical Engineering & Physics* **35**, 96–102.

Sevick JL, Abusara Z, Andrews SH, et al. (2018) Fibril Deformation Under Load of the Rabbit Achilles Tendon and Medial Collateral Ligament Femoral Entheses. *J Orthop Res* **36**, 2506–2515.

Shearer T, Rawson S, Castro SJ, et al. (2014) X-ray computed tomography of the anterior cruciate ligament and patellar tendon. *Muscles, ligaments and tendons journal* **4**, 238.

Sherman VR, Yang W, Meyers MA (2015) The materials science of collagen. *Journal of the Mechanical Behavior of Biomedical Materials* **52**, 22–50.

Silver FH, Freeman JW, Seehra GP (2003) Collagen self-assembly and the development of tendon mechanical properties. *Journal of Biomechanics* **36**, 1529–1553.

Sombke A, Lipke E, Michalik P, et al. (2015) Potential and limitations of X-Ray micro-computed tomography in arthropod neuroanatomy: A methodological and comparative survey: Micro-CT in Arthropod Neuroanatomy. *Journal of Comparative Neurology* **523**, 1281–1295.

Spalazzi JP, Gallina J, Fung-Kee-Fung SD, et al. (2006) Elastographic imaging of strain distribution in the anterior cruciate ligament and at the ligament–bone insertions. *Journal of Orthopaedic Research* **24**, 2001–2010.

Stabile KJ, Pfaeffle J, Weiss JA, et al. (2004) Bi-directional mechanical properties of the human forearm interosseous ligament. *Journal of Orthopaedic Research* **22**, 607–612.

Starborg T, Kalson NS, Lu Y, et al. (2013) Using transmission electron microscopy and 3View to determine collagen fibril size and three-dimensional organization. *Nature Protocols* **8**, 1433–1448.

Starborg T, Lu Y, Huffman A, et al. (2009) Electron microscope 3D reconstruction of branched collagen fibrils *in vivo*. *Scandinavian Journal of Medicine & Science in Sports* **19**, 547–552.

Stark H, Fröber R, Schilling N (2013) Intramuscular architecture of the autochthonous back muscles in humans. *J Anat* **222**, 214–222.

Stark H, Schilling N (2010) A novel method of studying fascicle architecture in relaxed and contracted muscles. *Journal of Biomechanics* **43**, 2897–2903.

Stouffer DC, Butler DL, Hosny D (1985) The Relationship Between Crimp Pattern and Mechanical Response of Human Patellar Tendon-Bone Units. *Journal of Biomechanical Engineering* **107**, 158.

Sullivan SP, McGechie FR, Middleton KM, et al. (2019) 3D Muscle Architecture of the Pectoral Muscles of European Starling (*Sturnus vulgaris*). *Integrative Organismal Biology* **1**.

Svensson RB, Herchenhan A, Starborg T, et al. (2017) Evidence of structurally continuous collagen fibrils in tendons. *Acta Biomaterialia* **50**, 293–301.

Szczesny SE, Elliott DM (2014) Interfibrillar shear stress is the loading mechanism of collagen fibrils in tendon. *Acta Biomaterialia* **10**, 2582–2590.

Thambyah A, Lei Z, Broom N (2014) Microanatomy of the Medial Collateral Ligament Enthesis in the Bovine Knee. *Anat Rec (Hoboken)* **297**, 2254–2261.

Thomopoulos S, Parks WC, Rifkin DB, et al. (2015) Mechanisms of tendon injury and repair. *J Orthop Res* **33**, 832–839.

Thomopoulos S, Williams GR, Gimbel JA, et al. (2003) Variation of biomechanical, structural, and compositional properties along the tendon to bone insertion site. *Journal of Orthopaedic Research* **21**, 413–419.

Thorpe CT, Godinho MSC, Riley GP, et al. (2015) The interfascicular matrix enables fascicle sliding and recovery in tendon, and behaves more elastically in energy storing tendons. *Journal of the Mechanical Behavior of Biomedical Materials* **52**, 85–94.

Thorpe CT, Klemt C, Riley GP, et al. (2013) Helical sub-structures in energy-storing tendons provide a possible mechanism for efficient energy storage and return. *Acta Biomaterialia* **9**, 7948–7956.

Thorpe CT, Udeze CP, Birch HL, et al. (2012) Specialization of tendon mechanical properties results from interfascicular differences. *J R Soc Interface* **9**, 3108–3117.

Tozzi G, Peña Fernández M, Davis S, et al. (2020) Full-Field Strain Uncertainties and Residuals at the Cartilage-Bone Interface in Unstained Tissues Using Propagation-Based Phase-Contrast XCT and Digital Volume Correlation. *Materials* **13**, 2579.

Turcotte CM, Green DJ, Kupczik K, et al. (2020) Elevated activity levels do not influence extrinsic fiber attachment morphology on the surface of muscle attachment sites. *J Anat* **236**, 827–839.

Vidal B de C, dos Anjos EHM, Mello MLS (2015) Optical anisotropy reveals molecular order in a mouse enthesis. *Cell and Tissue Research* **362**, 177–185.

Villegas DF, Maes JA, Magee SD, et al. (2007) Failure properties and strain distribution analysis of meniscal attachments. *Journal of Biomechanics* **40**, 2655–2662.

Vogel KG, Koob TJ (1989) Structural Specialization in Tendons under Compression. *International Review of Cytology* **115**, 267–293.

Waggett AD, Ralphs JR, Kwan APL, et al. (1998) Characterization of collagens and proteoglycans at the insertion of the human Achilles tendon. *Matrix Biol* **16**, 457–470.

Walters M, Crew M, Fyfe G (2019) Bone Surface Micro Topography at Craniofacial Entheses: Insights on Osteogenic Adaptation at Muscle Insertions. *Anat Rec* **302**, 2140–2155.

Walton LA, Bradley RS, Withers PJ, et al. (2015) Morphological Characterisation of Unstained and Intact Tissue Micro-architecture by X-ray Computed Micro- and Nano-Tomography. *Scientific Reports* **5**, 10074.

Wang JH-C (2006) Mechanobiology of tendon. *Journal of Biomechanics* **39**, 1563–1582.

Wang M, Van Houten JN, Nasiri AR, et al. (2013) PTHrP regulates the modeling of cortical bone surfaces at fibrous insertion sites during growth. *J Bone Miner Res* **28**, 598–607.

Welsch U, Mulisch M (2010) *Romeis Mikroskopische Technik*, Heidelberg: Spektrum Akademischer Verlag.

Wilde F, Ogurreck M, Greving I, et al. (2016) Micro-CT at the imaging beamline P05 at PETRA III. In Proceedings of the 12th International Conference on Synchrotron Radiation Instrumentation – SRI2015. New York, NY USA, 030035.

Wilkins SW, Nesterets YI, Gureyev TE, et al. (2014) On the evolution and relative merits of hard X-ray phase-contrast imaging methods. *Philosophical Transactions of the Royal Society A* **372**, 20130021.

Wopenka B, Kent A, Pasteris JD, et al. (2008) The tendon-to-bone transition of the rotator cuff: a preliminary Raman spectroscopic study documenting the gradual mineralization across the insertion in rat tissue samples. *Applied spectroscopy* **62**, 1285–1294.

Wren TA, Beaupre GS, Carter DR (2000) Mechanobiology of tendon adaptation to compressive loading through fibrocartilaginous metaplasia. *Journal of rehabilitation research and development* **37**, 135.

Yu SM, Yu JS (2015) Calcaneal Avulsion Fractures: An Often Forgotten Diagnosis. *American Journal of Roentgenology* **205**, 1061–1067.

Zhao L, Thambyah A, Broom ND (2014) A multi-scale structural study of the porcine anterior cruciate ligament tibial enthesis. *Journal of Anatomy* **224**, 624–633.

Supplement

Table of contents

Supplement 1

Three-dimensional imaging of the fibrous microstructure of Achilles tendon entheses in Mus musculus

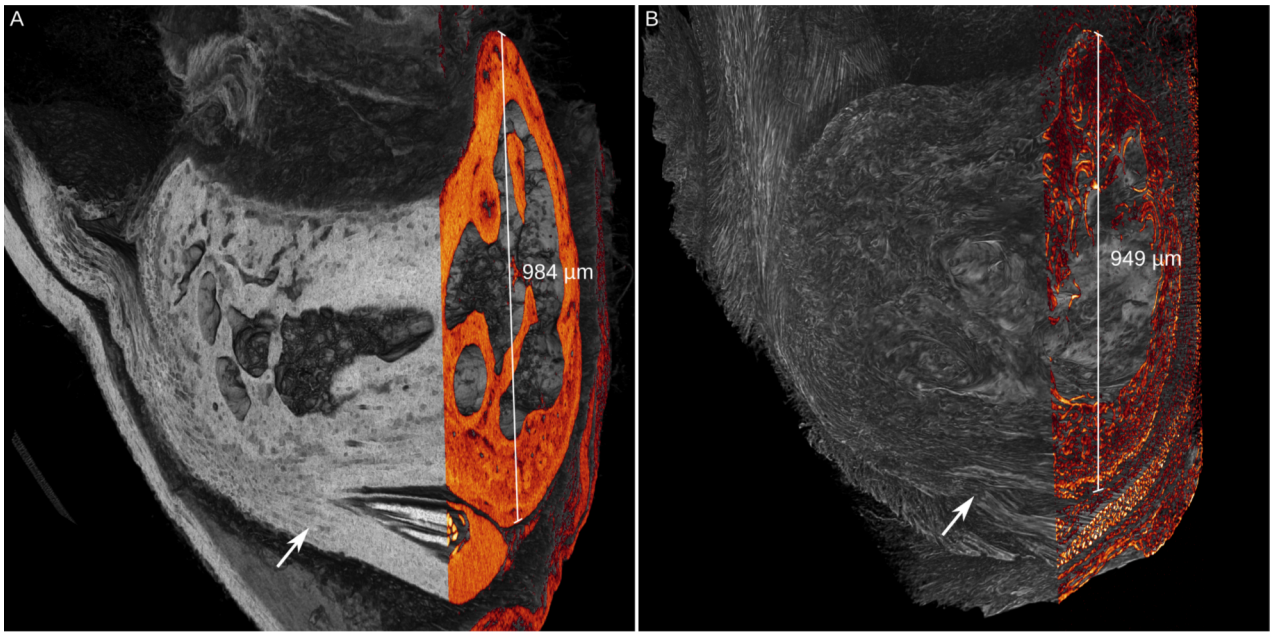

Fig. S1: Calcaneus height was measured between the plantar periosteum anterolateral from the origin (arrows) of the M. abductor brevis digiti minimi on the one hand and the periosteum of the dorsal ridge of the Calcaneus neck on the other, as demonstrated in volume renderings of (A) the demineralized and PTA-stained Achilles tendon enthesis (scan no. 4) and (B) a fibrous structure specimen (scan no. 6).

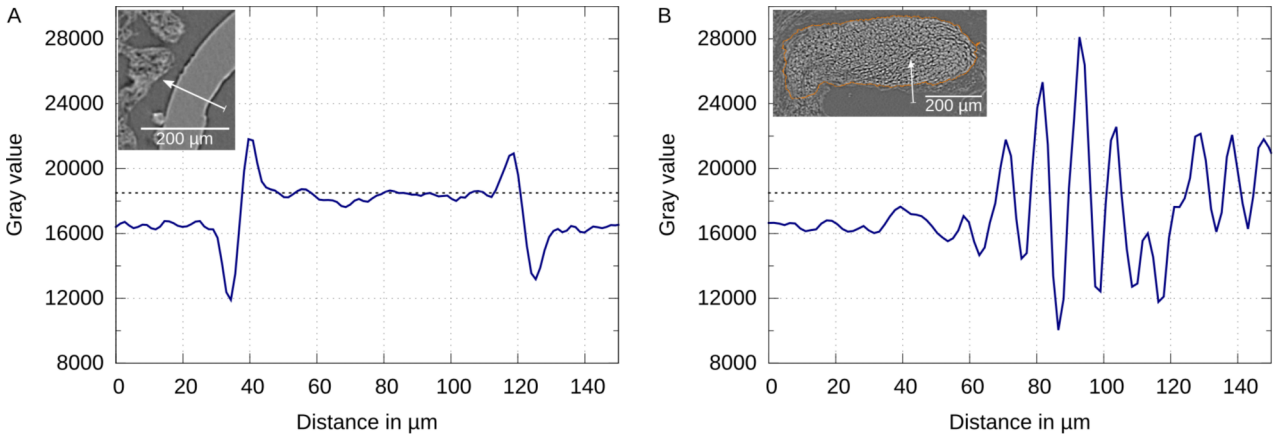

Fig. S2: Gray value profiles along lines in a fibrous structure volume image (scan no. 6). (A) Phase-contrast fringes at the transition between air and hot-melt adhesive each comprise a gray value minimum within air and a maximum within hot-melt adhesive, while homogeneous materials at a distance from the transitions are represented by plateaus. (B) Within collagen fibers, the gray values do not go back to a plateau. The profile through each single tendon fiber is unimodal. Insets show sections from the fibrous structure volume with the positions of the line profiles.

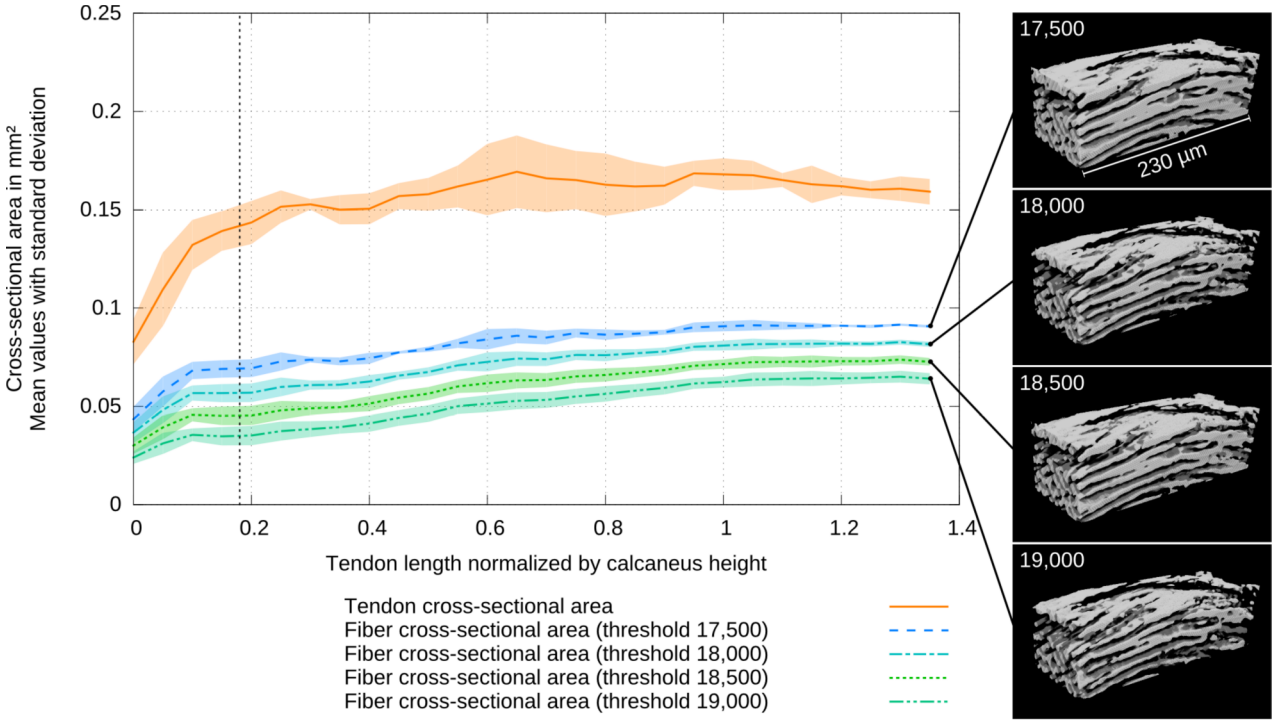

Fig. S3: Diagram of fiber cross-sectional area over normalized tendon length for four different gray value thresholds. Tendon cross-sectional area is given as a reference.

Supplement 2

Tracking tendon fibers to their insertion – a 3D analysis of the Achilles tendon enthesis in mice

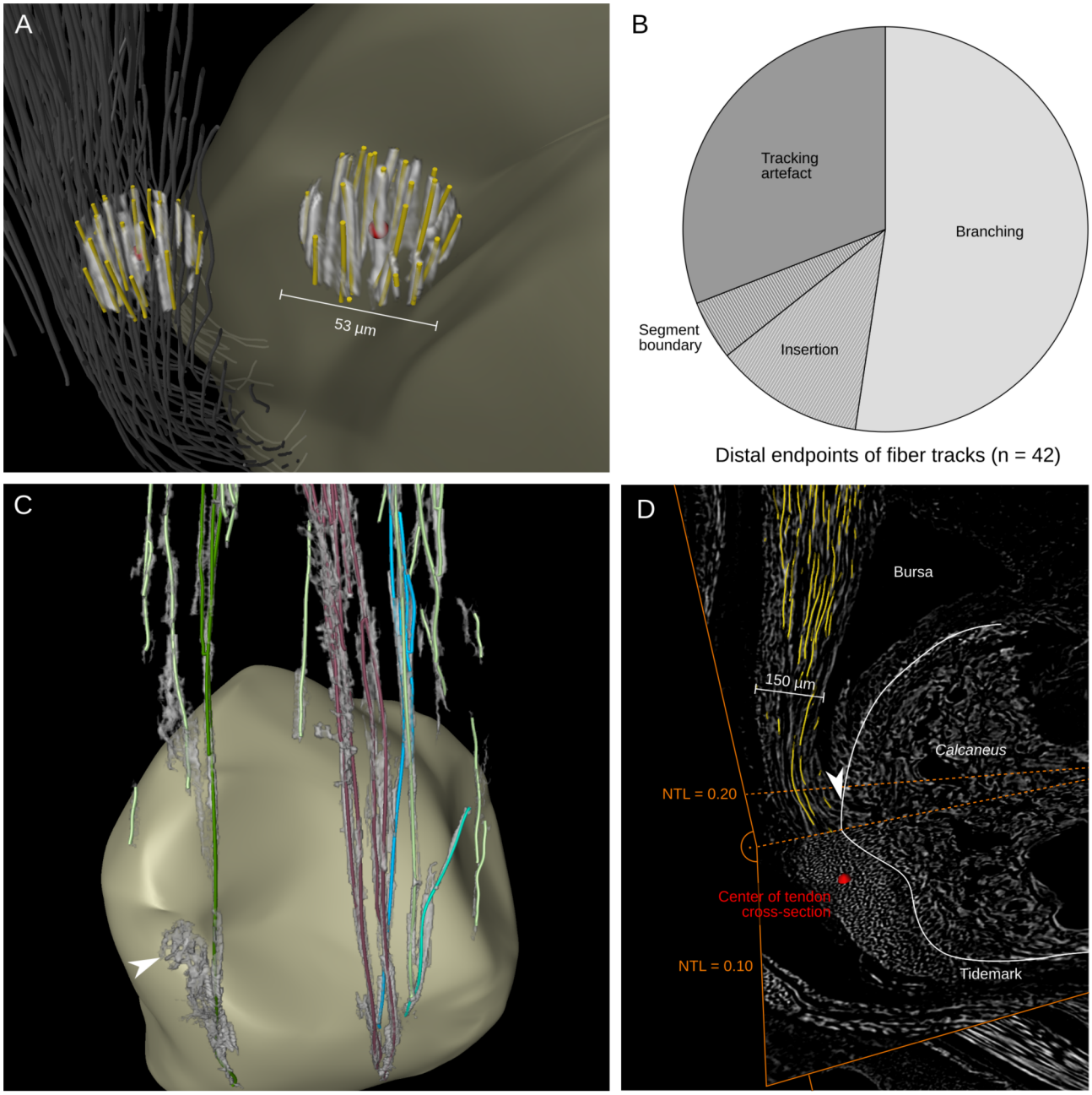

Fig. S1: Evaluation of fiber tracks, endpoints, and branching. (A) Spheres of the volume data and the fiber tracks were extracted around endpoints of fiber tracks in order to evaluate them. (B) Accordingly, a sample of distal endpoints of fiber tracks (n = 42) was classified into categories. The majority of these endpoints correspond to branching points. (C) A rendering of clusters of fiber tracks with the corresponding segments of the volume data shows that distally larger regions are attributed to a cluster (arrowhead). (D) A rendering of fiber tracks together with a sagittal and a transversal slice shows that the proximal-most position where fibers insert (arrowhead) corresponds to an NTL of 0.18.

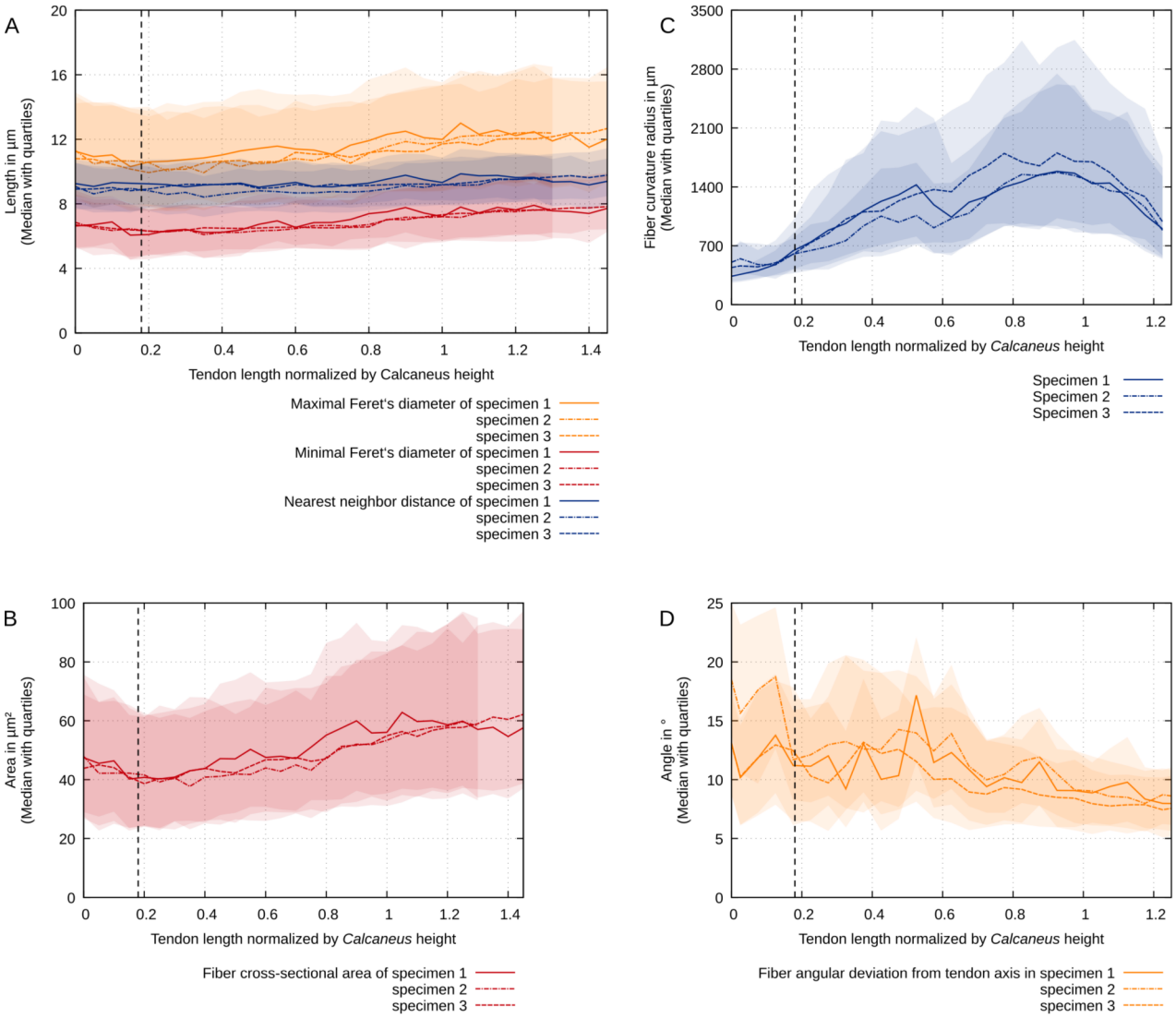

Fig. S2: Fiber sizes, curvatures and orientations over all three specimens. (A) The medians of the maximal and the minimal Feret's diameter of the fibers in all three specimens decrease towards the insertion. The median nearest neighbor distance of the centroids of the fiber masks stays about constant over the NTL. (B) The median CSA of the fibers decreases towards the insertion. (C) The median curvature radius is maximal around an NTL of 0.90. It decreases towards the proximal end of the dataset and the insertion, where minimal radii are measured. (D) The median angular deviation of fiber vectors from the mid-tendon line is higher near the insertion than at the proximal end of the dataset.

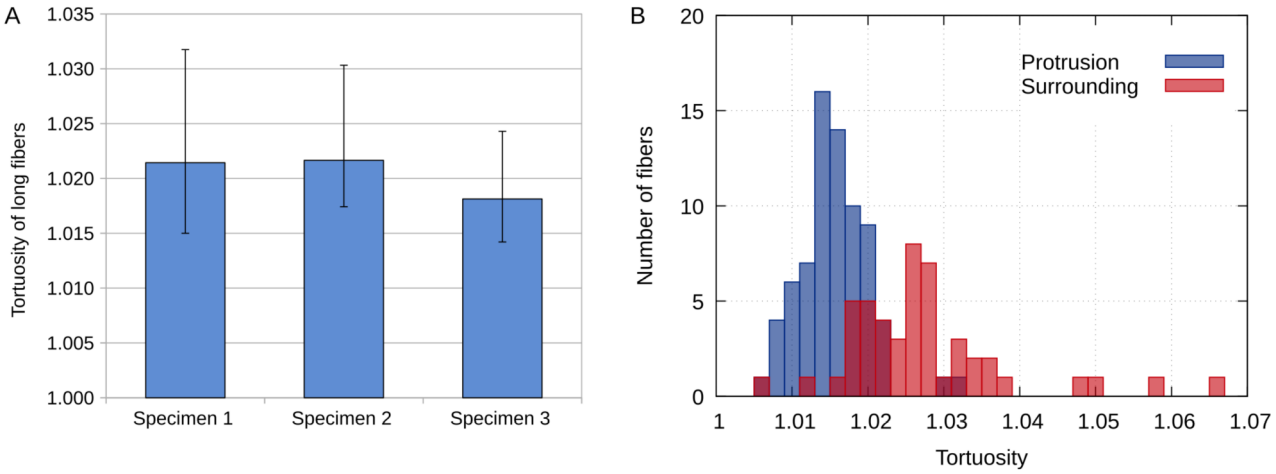

Fig. S3: Tortuosity. (A) Median tortuosities with quartiles of all three specimens. (B) Frequency of tortuosities among fibers of the protrusion and surrounding fibers in specimen 3.

Supplement 3

Gaining insight into the deformation of Achilles tendon entheses in mice

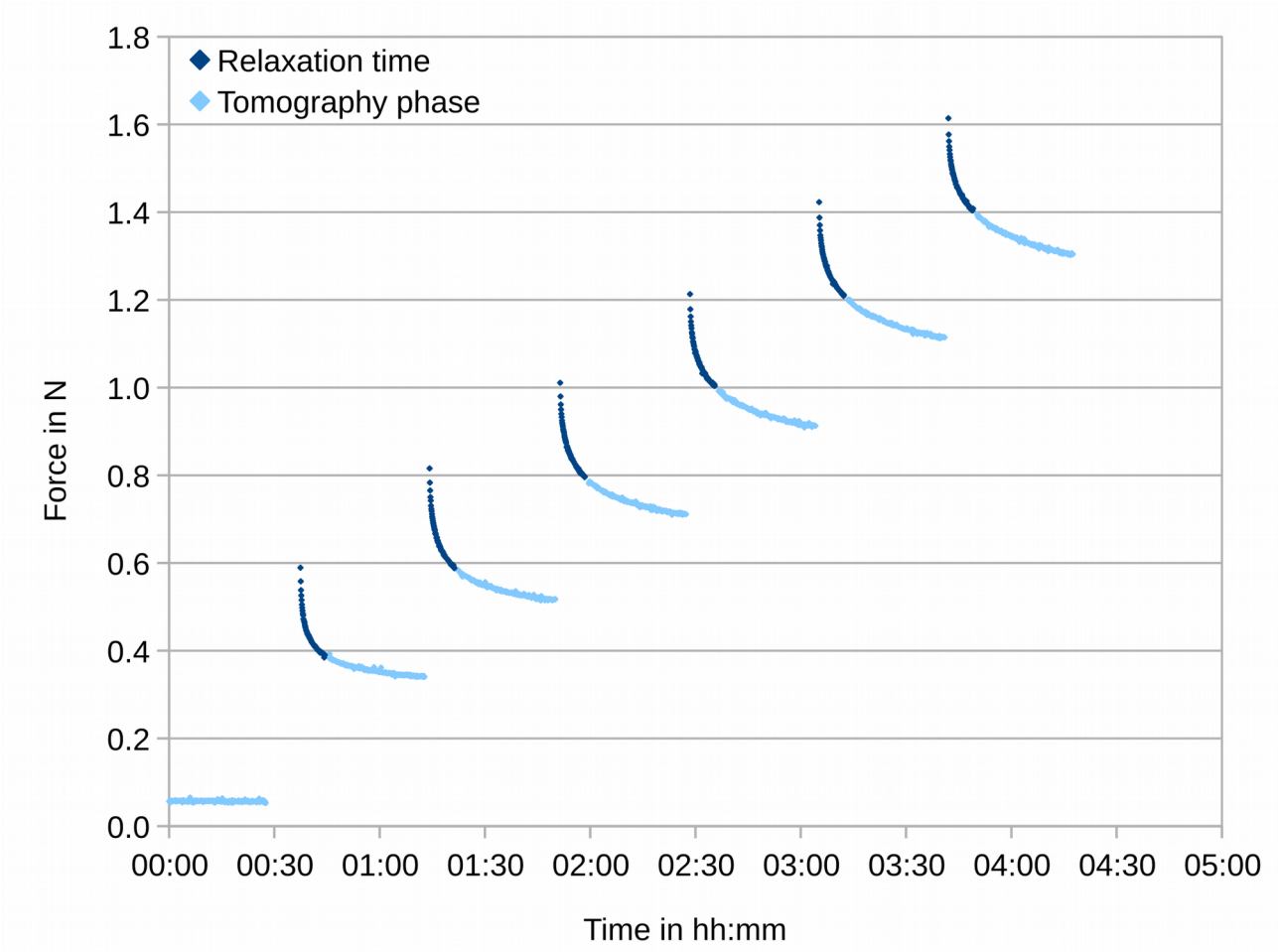

Fig. S1: Force diagram of a specimen tested in a force program without being exposed to synchrotron X-ray radiation during the tomography phases.

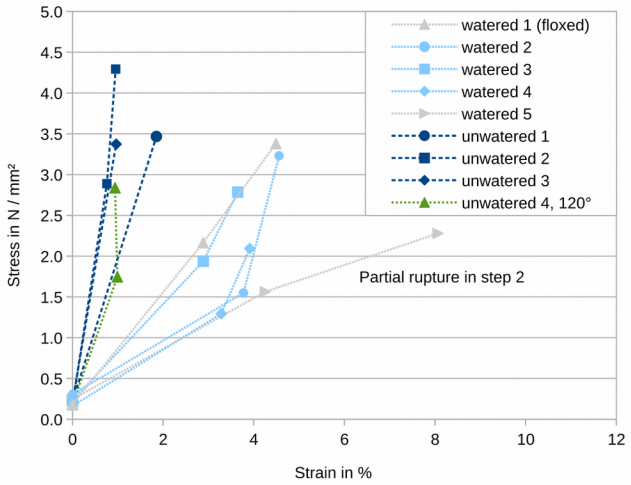

Fig. S2: Stress over strain for the total test distance in the individual specimens. If data from two force steps was available, it is plotted.

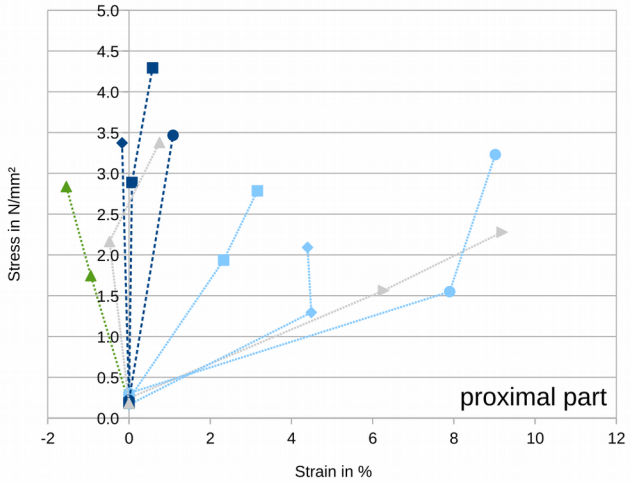

Fig. S3: Stress over strain for the proximal part of the test distance in the individual specimens. If data from two force steps was available, it is plotted. The legend corresponds to figure S2.

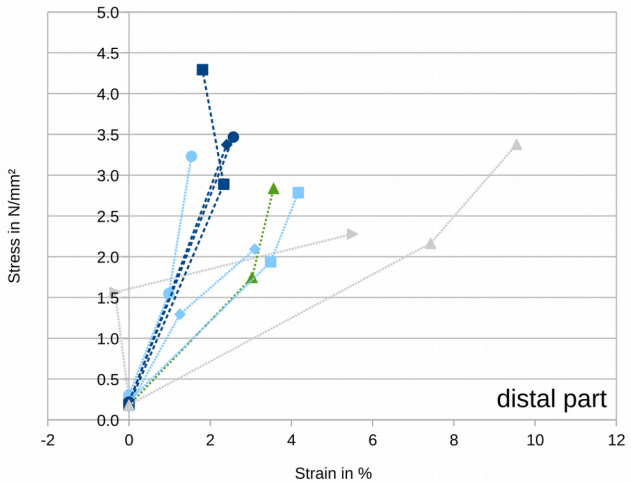

Fig. S4: Stress over strain for the distal part of the test distance in the individual specimens. If data from two force steps was available, it is plotted. The legend corresponds to figure S2.

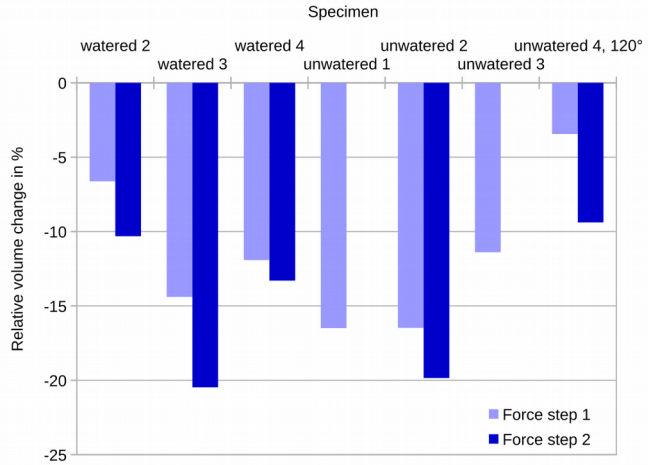

Fig. S5: Relative volume changes of the examined part of the tendon in the individual specimens measured after the first force step and if possible after the second one.

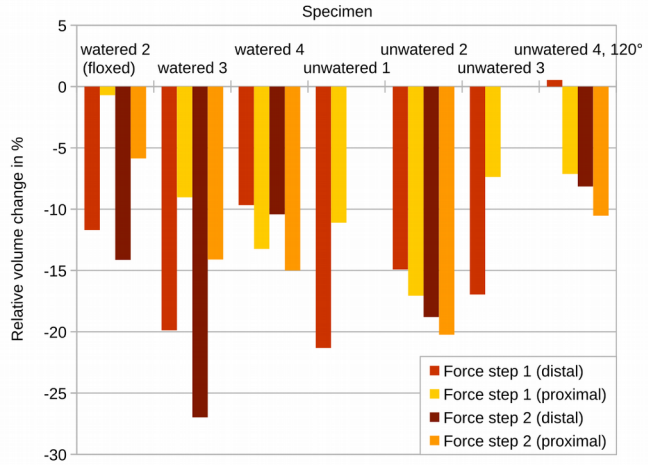

Fig. S6: Relative volume changes of the proximal and distal part of the examined volume in the individual specimens measured after the first force step and if possible after the second one.

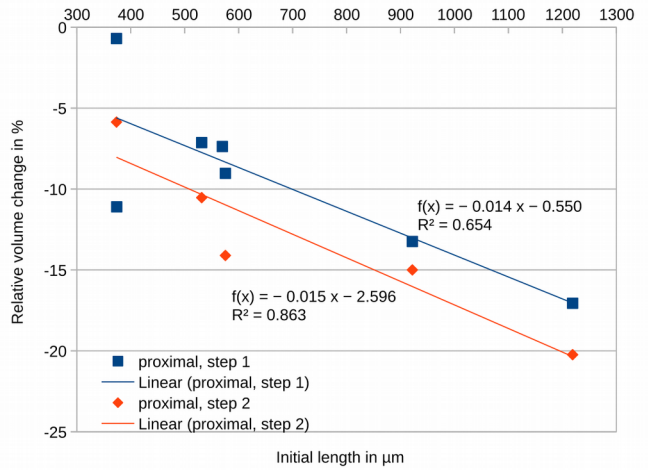

Fig. S7: Relative volume changes in the proximal part over initial length of the proximal test distance. The further the proximal test distance extends into the free tendon, the larger is the decrease in volume in the examined force steps.

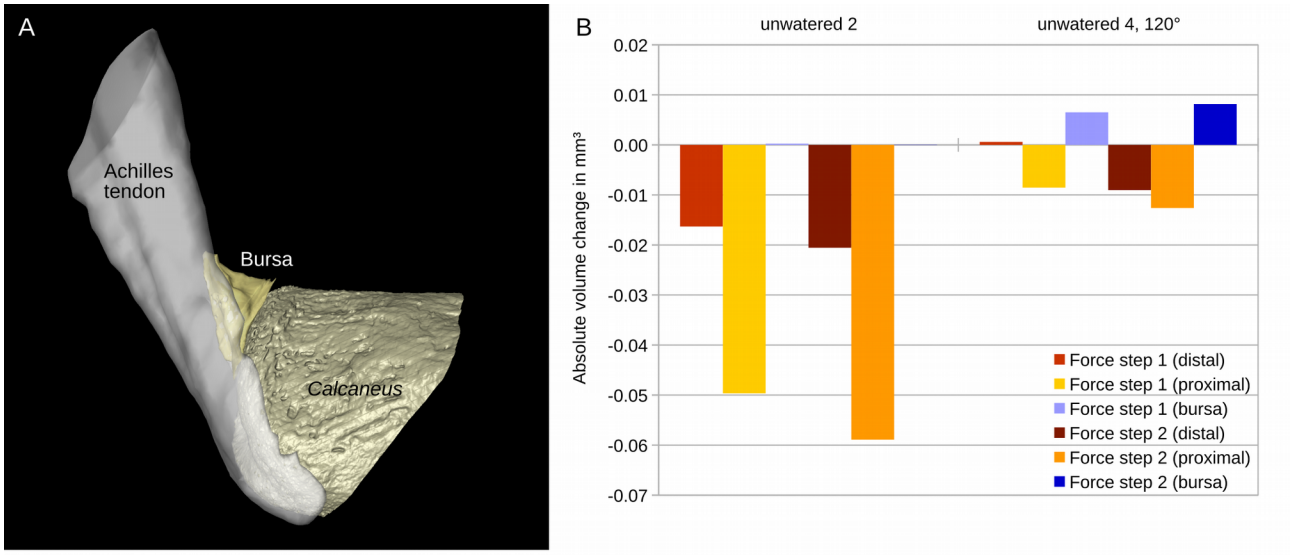

Fig. S8: The bursa. (A) Surface rendering of bone, tendon and bursa. (B) Absolute volume changes of tendon and bursa at nominal insertion angles of 90° and 120°. Each angle is examined in one specimen.

Ehrenwörtliche Erklärung

Hiermit erkläre ich, dass mir die geltende Promotionsordnung der Fakultät für Biowissenschaften der Friedrich-Schiller-Universität Jena bekannt ist,

ich die Dissertation selbst angefertigt habe, keine Textabschnitte eines Dritten oder eigener Prüfungsarbeiten ohne Kennzeichnung übernommen habe und alle von mir benutzten Hilfsmittel, persönlichen Mitteilungen und Quellen in meiner Arbeit angegeben sind,

mich folgende Personen bei der Auswahl und Auswertung des Materials sowie bei der Herstellung des Manuskripts unterstützt haben: Heiko Stark, Sebastian Köhring, Jörg U. Hammel, Markus Löffler, Hartmut Witte, Martin S. Fischer,

die Hilfe einer kommerziellen Promotionsvermittlung nicht in Anspruch genommen wurde und dass Dritte weder unmittelbar noch mittelbar geldwerte Leistungen von mir für Arbeiten erhalten haben, die im Zusammenhang mit dem Inhalt der vorgelegten Dissertation stehen,

dass ich die Dissertation noch nicht als Prüfungsarbeit für eine staatliche oder andere wissenschaftliche Prüfung eingereicht habe und

dass ich die gleiche, eine in wesentlichen Teilen ähnliche oder eine andere Abhandlung nicht bei einer anderen Hochschule als Dissertation eingereicht habe.

Datum _____ Unterschrift des Verfassers _____